DEC -7 2005

REPORT DOCUMENTATION PAGE

Form Approved
OMB No. 0704-0188

1. REPORT DATE	2. REPORT TYPE	3. DATES COVERED
12-1-2005	Final Report	1st April 2002 to 31st Dec 2005

4. TITLE AND SUBTITLE
AIR EJECTOR PUMPING ENHANCEMENT THROUGH PULSING PRIMARY FLOW

5a. CONTRACT NUMBER
F49620-02-1-0131

5b. GRANT NUMBER

5c. PROGRAM ELEMENT NUMBER

6. AUTHOR(S)
Peter J. Vermeulen, Venkataramanayya Ramesh, Guang Cai Meng

Daniel N. Miller and Neal Domel.

5d. PROJECT NUMBER

5e. TASK NUMBER

5f. WORK UNIT NUMBER

7. PERFORMING ORGANIZATION NAME(S) AND ADDRESS(ES)

Department of Mechanical Engineering
University of Calgary
2500 University Drive NW
Calgary, Alberta T2N 1N4
CANADA.

8. PERFORMING ORGANIZATION REPORT NUMBER

9. SPONSORING / MONITORING AGENCY NAME(S) AND ADDRESS(ES)
Air Force Office of Scientific
Research , USAF

10. SPONSOR/MONITOR'S ACRONYM(S)
AFOSR

11. SPONSOR/MONITOR'S REPORT NUMBER(S)

12. DISTRIBUTION / AVAILABILITY STATEMENT

DISTRIBUTION STATEMENT A
Approved for Public Release
Distribution Unlimited

13. SUPPLEMENTARY NOTES

14. ABSTRACT Improving the performance of an ejector is a flow control problem. Passive methods such as changing the geometry of the mixing tube showed that, for a simple mixing tube geometry of a concentric cone-tube combination, the diameter of the tube had to be at least 4 times the diameter of the primary nozzle. Thus for a 5.13 mm dia. primary jet, a 22.7 mm dia. tube was 27% better than a 17.41 mm dia. tube. A standard Venturi mixing tube with 17.41 mm dia. throat was 100% better. Also the shape of the entrance cone had only a little effect and could be substituted by other shapes. A tube without an entrance shape was found to be still reasonably efficient.

Both experiments and Computer Fluid Dynamics(CFD) analysis show that pulsing the primary jet flow, an active method of flow control, improved ejector performance. The physics of this improvement has been discussed. Pumping effectiveness of the ejector was found to be proportional to the square of the pulsation strength. The details of the many pulsators tested are discussed. The majority of the improvement appears to be due to the initial toroidal vortex, the pulsation produces. The improvement was strongest at 127-131 Hz, less than half the fundamental frequency of 746 Hz of the system. The pumping effectiveness increased by up to 4.5 times that for a steady jet. Different types of pulse shapes tested indicate that a sinusoidal pulse superimposed on a steady flow is very efficient. For pulses which have only positive pulse velocities, a narrow pulse was more efficient. The data also showed that a strong synthetic jet actuator gave ejector performance as good as a pulsed jet with primary flow.

15. SUBJECT TERMS

16. SECURITY CLASSIFICATION OF:			17. LIMITATION OF ABSTRACT	18. NUMBER OF PAGES	19a. NAME OF RESPONSIBLE PERSON
a. REPORT	b. ABSTRACT	c. THIS PAGE		30 pages	V.Ramesh

19b. TELEPHONE NUMBER *(include area code)* 403 220 8730
E-Mail viyya@yahoo.com

Standard Form 298 (Rev. 8-98)
Prescribed by ANSI Std. Z39.18

20060103 117

AIR FORCE OFFICE OF SCIENTIFIC RESEARCH

DTIC Data

Purchase Request Number: FQ8671-0200548

BPN:

Proposal Number: 01-NA-187

Type Submission: ~~New Work Effort~~ Final Report

Inst. Control Number: F49620-02-1-0131DEF

Institution: UNIV OF CALGARY

Primary Investigator: Prof. Peter J. Vermeulen

Invention Ind: none

Project/Task: 2307B / X

Program Manager: Rhett W. Jefferies

Objective:

The objective of the proposed work is to conduct research into using acoustically driven or pulsed ejectors capable of pumping increased secondary flows in ejector assemblies. Previous research has demonstrated that increased entrainment is possible in pulsed ejector designs, and the current research project will further investigate the mechanisms for this augmentation.

Approach:

An existing test rig will be used to conduct research establishing the geometry, pulsing frequencies, and amplitudes for optimum ejector efficiency. Complementary computational studies will be performed to further investigate the mechanisms by which additional entrainment is achieved in these configurations.

Progress:

Year: 2004 **Month:**

The performance of an ejector with a 5 mm dia. nozzle, pulsed by a loudspeaker acoustic driver, showed that pulsing tl primary flow increased the pumping effectiveness ratio (P.E.R) by four times, consistent with data reported for the 10 mm dia. nozzle ejector. Varying the throat spacing showed that the mixing tube entry cone augmented the mixing process. This is part of the objective of optimizing the ejector geometry which will be continued by varying the mixing tube entry and diffuser geometry. This ejector was also successfully pulsed by a newly developed disc rotor valve pulsator to meet the objective of operation at practical Mach numbers. Specifically a P.E.R. of 1.2 was obtained at an average jet Mach number M~ =0.76, with a high pulse Mach number Mh = 0.93, at 131 Hz. By manipulating the velocit time pulse shape a P.E.R. of 1.7 was obtained at =
0.33, and Mb = 0.75, at 120 Hz. Further development should reach the target P.E.R. of 2, at a high average jet subson Mach number, by pulsing to low supersonic speeds. Measurements of secondary (entrainment) air mass flow rate, pulsed at 131 Hz for zero jet velocity, showed a powerful synthetic jet actuator could give a similar performance to a pulsed high velocity jet.

Year: 2005 **Month:** 12 **Final**

Final Report: 01 Mar 2002 - 31 Dec 2004

Improving the performance of an ejector is a flow control problem. Passive methods such as changing the geometry o the mixing tube showed that, for a simple mixing tube geometry of a concentric cone-tube combination, the diameter o

Progress:

Year: 2005 **Month:** 12 **Final**

the tube had to be at least 4 times the diameter of the primary nozzle. Thus for a 5.13 mm dia. primary jet, a 22.7 mm dia. tube was 27% better than a 17.41 mm dia. tube. A standard Venturi mixing tube with 17.41 mm dia. throat was 100% better. Also the shape of the entrance cone had only a little effect and could be substituted by other shapes. A tube without an entrance shape was found to be still reasonable efficient.

Both experiments and Computer Fluid Dynamics(CFD) analysis show that pulsing the primary jet flow, an active metho of flow control, improved ejector performance. The physics of this improvement has been discussed. Pumping effectiveness of the ejector was found to be proportional to the square of the pulsation strength. The details of the mar pulsators tested are discussed. The majority of the improvement appears to be due to the initial toroidal vortex, the pulsation produces. The improvement was strongest at 127-131 Hz, less than half the fundamental frequency of 746 H of the system. The pumping effectiveness increased by up to 4.5 times that for a steady jet. Different types of pulse shapes tested indicate that a sinusoidal pulse superimposed on a steady flow is very efficient. For pulses which have only positive pulse velocities, a narrow pulse was more efficient. The data also showed that a strong synthetic jet actuator gave ejector performance as good as a pulsed jet with primary flow.

EJECTOR PUMPING ENHANCEMENT THROUGH PULSING PRIMARY FLOW

AFOSR GRANT NO.F49620-02-1-0131

Peter.J.Vermeulen*

Venkataramanayya Ramesh**

Guang Cai Meng***
Department of Mechanical and Manufacturing Engineering
University of Calgary, Calgary, Alberta, Canada

Daniel N. Miller and Neal Domel****
Lockheed Martin Aeronautics Company, Propulsion Systems and CFD Technologies
Fort Worth, Texas,MZ 9333

Abstract

Improving the performance of an ejector is a flow control problem. Passive methods such as changing the geometry of the mixing tube showed that, for a simple mixing tube geometry of a concentric cone-tube combination, the diameter of the tube had to be at least 4 times the diameter of the primary nozzle. Thus for a 5.13 mm dia. primary jet, a 22.7 mm dia. tube was 27% better than a 17.41 mm dia. tube. A standard Venturi mixing tube with 17.41 mm dia. throat was 100% better. Also the shape of the entrance cone had only a little effect and could be substituted by other shapes. A tube without an entrance shape was found to be still reasonably efficient.

Both experiments and Computer Fluid Dynamics(CFD) analysis show that pulsing the primary jet flow, an active method of flow control, improved ejector performance. The physics of this improvement has been discussed. Pumping effectiveness of the ejector was found to be proportional to the square of the pulsation strength. The details of the many pulsators tested are discussed. The majority of the improvement appears to be due to the initial toroidal vortex, the pulsation produces. The improvement was strongest at 127-131 Hz, less than half the fundamental frequency of 746 Hz of the system. The pumping effectiveness increased by up to 4.5 times that for a steady jet. Different types of pulse shapes tested indicate that a sinusoidal pulse superimposed on a steady flow is very efficient. For pulses which have only positive pulse velocities, a narrow pulse was more efficient. The data also showed that a strong synthetic jet actuator gave ejector performance as good as a pulsed jet with primary flow.

Nomenclature

Ce	= Entrainment Coefficient
CFD	= Computational Fluid Dynamics
CL	= centre-line
D	= diameter
f	= driving frequency
I	= electric current to the loudspeaker acoustic driver
K	= a constant
L	= length
M	= Mach number
$\overline{Mj}$	= average jet Mach number
Mp	= primary jet mass flow rate
Ms	= secondary (entrainment) mass flow rate

---

* Dr. P.J.Vermeulen, sadly passed away on 20 Dec 2004.
** Research Associate, Mechanical and Manufacturing Engineering.
*** Part Time Graduate Student, To defend thesis on 14 Jan 2005, Presently employed .
**** Senior Engineering Staff, Propulsion Systems.

M_T = total mass flow rate (Mp+Ms)
ND = "no drive"
P = static pressure
P.E. = pumping effectiveness
P.E.D. = dimensionless pumping effectiveness parameter
P.E.R. = pumping effectiveness ratio
Po = stagnation pressure
$\overline{Poj}$ = jet flow average stagnation pressure
R = specific gas constant
R.V.P. = rotor valve pulsator
Re = jet flow Reynolds number (ND)
S = throat spacing-distance between mixing tube throat and nozzle exit plane
St = $fDj/\overline{Uj}$ jet Strouhal number based on $\overline{Uj}$
To = stagnation temperature
UeCL = Ue-UjCL
Uh = maximum velocity of the pulse on centre-line
UjCL = average jet velocity at centre-line of nozzle
$\overline{Uj}$ = average jet flow velocity calculated from Mp(ND)
V = voltage across loudspeaker acoustic driver
We = electric power into loudspeaker acoustic driver
Wa = acoustic power input to primary jet flow to pulsate
WD = "with drive"

Greek Symbols

ρ = flow density

Subscripts

a = atmosphere
h,H =maximum value
j = jet flow at nozzle orifice exit plane
L = low value
m =mixing tube

Introduction

An ejector is made up of a primary jet of fluid of mass flow rate Mp, which entrains the surrounding fluid. The primary jet and the entrained fluid mix in the mixing tube and are ejected out. If the surroundings are confined to a chamber, the pressure in the chamber decreases which requires a secondary flow of fluid of mass flow rate Ms, equal to the entrained fluid to prevent the pressure from dropping.

Ejectors have been used in many ways, from creating vacuum to changing thrust vectors in VTOL and STOL aircraft. As an ejector has no moving parts it can be used to evacuate engine bays and such other cavities in the vicinity of the engine where hot gases may accumulate and affect engine performance. In the realm of fluidic nozzles an ejector can deflect the thrust vector.

Previous work has shown that pulsing the primary flow[1,2,3,4] in an ejector increases both entrainment as well as mixing. Thrust augmentation up to twice steady flow thrust has been achieved in pulse jet engines [5]. Usually Hartmann and Sprenger tube pulsators are used and appear to give good amplitude of pulsation. These pulsators employ shock waves to reduce supersonic flow to pulsed subsonic flow. The losses of such a mechanism is expected to be very high.

Experiments on pulsing primary, secondary and tertiary air flows in combustors were carried out in this laboratory and showed that mixing was enhanced, leading to temperature changes at the exit of the combustor. A reduction in Nox was also measured [6] . Mixing of steady jet flows with confined cross flow, e.g.,Haldemann and Walker [7] and recent development of this work [8,9] showed that for a pulsed jet the mixing was significantly better and

a 100% increase in jet penetration. Majority of this work used a loudspeaker acoustic driver because of the ease with which frequency and amplitude could be controlled. However sirens and rotor valve pulsators which both use the same principle to pulse air have also been used in mixing and entrainment experiments [10].

It is evident that any improvement in the performance of an ejector would be very beneficial. For example, in evacuating engine bays, high pressure air for the primary jet is bled from the compressor. If pulsing this flow could reduce the amount bled, the penalty on engine performance would be reduced. In thrust vectoring [15,16,17] and pulse jet engines, if pulsing of primary air can achieve the same effect with a smaller jet flow as a steady jet, then the ejectors can be smaller in size and more economical

Increasing the entrainment by the primary jet falls into the category of flow control. Flow control involves passive and active methods to affect a beneficial change. Changing the size of the primary nozzle, a passive method, does not appear to change the performance in a significant way. Thus from previous experiments, for the same velocity of primary flow, a 10.03 mm dia. nozzle gave a pumping effectiveness P.E. value of 0.62-0.7 while a 5.13 mm dia. nozzle gave P.E. of 2.7-2.8. Since Mp for the bigger nozzle is 4 times that for the smaller one, the difference in P.E. value just shows that Ms, the entrained flow rate is the same for both the nozzles. Changing the geometry of the mixing tube is also a passive method to optimize the ejector performance. Results are given of tests conducted on a 5.13mm dia. primary nozzle jet going into a cylindrical mixing tube of 17.41mm dia. with 21°,30° and 40° entrance cones; into a cylindrical mixing tube of 22.7mm dia. with a 40° entrance cone and into a 21° contraction and 12° diffuser Venturi mixing tube with a 17.41 mm dia. throat.

Active methods of flow control involve changing the character of the primary flow. This can be done in various ways such as using different gases, changing the temperature and pulsing the flow. The present work deals only with the last method-pulsing the primary flow by the use of loudspeaker acoustic drivers with two recommended enclosures, disc rotor valve pulsators(R.V.P.) which are similar to sirens and consist mainly of a rotating disc with small openings which line up with the supply air pipe every rotation and allow air to pass through to the primary nozzle. Other pulsators investigated were the dumbbell type of oscillating piston device, side branch aero acoustic pulsator and a tube pulsator. A piston-cylinder pulsator was also tried. More details are given of these pulsators later. Results are given from experiments carried out with the loudspeaker, the R.V.P. and the piston-cylinder pulsator. A few tests were done with the dumbbell pulsator and results from those are also given. The side branch aero acoustic pulsator never gave any measurable pulsations. Unfortunately, due to time restrictions, only the pulsation characteristics of the tube-pulsator were investigated and these are given.

CFD results and discussion are given. These were made available in a private communication by Lockheed Martin Co. Ltd.

Description of Model

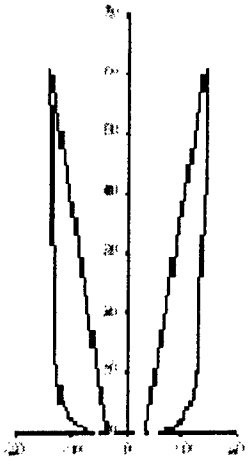

Fig. 1 Boundary Trace of Steady jet and Pulsed Jets

Figure 1 shows the trace of a free jet as determined by a hot film anemometer sweep at various distances downstream of the nozzle [11]. The axes are both in mm. The inner trace was for a steady jet and the outer, for a pulsed jet. The data was scaled from measurements made on a 9.53 mm dia. nozzle with $\overline{Uj}$=17.9 m/s, Ue=37.8 m/s at 250 Hz. The area inside this boundary multiplied by the average velocity at any given distance from the nozzle would in effect give the total volumetric flow at that point. Subtracting the jet flow from this would give the entrained mass flow rate. It is evident that the pulsed flow results in more entrained flow. It is noteworthy that the boundary area increases immediately downstream of the nozzle and then remains virtually constant till it crosses the steady jet boundary approximately 12 diameters downstream. This is attributed to the strong toroidal vortex at nozzle exit due to pulsation.

A vortex going past a hot film anemometer at the velocity of the jet gives a time-velocity trace as shown at the right end of figure 2. The velocity increases as the core of the vortex approaches, then the core rotating like a solid makes the velocity go down to zero. This repeats as the vortex centre goes past. As the anemometer is not sensitive to the direction of flow, an M-shaped trace results.

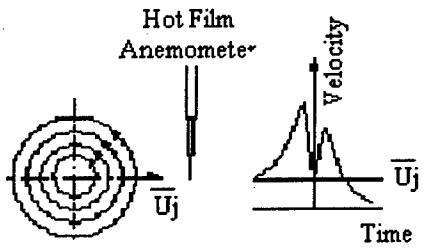

Fig. 2 Velocity Trace of a Vortex

This type of M-shaped traces obtained with a loudspeaker acoustic driver are shown in figure 3 for a range of $\overline{Uj}$'s and electrical power input to the loudspeaker driver. This experiment was coducted on a 5.13 mm dia. nozzle with a 40° cone, 22.7 mm dia. mixing tube.

These tests were conducted at a late stage of this project after Dr. Vermeulen was unable to work.

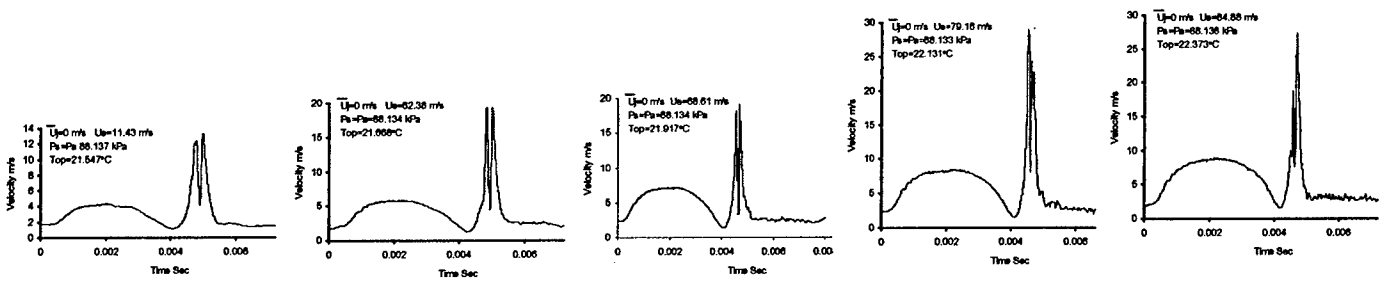

5.625 W | 22.638 W | 50.976 W | 101.17 W | 157.99 W

Primary Jet Velocity Uj=0 m/s

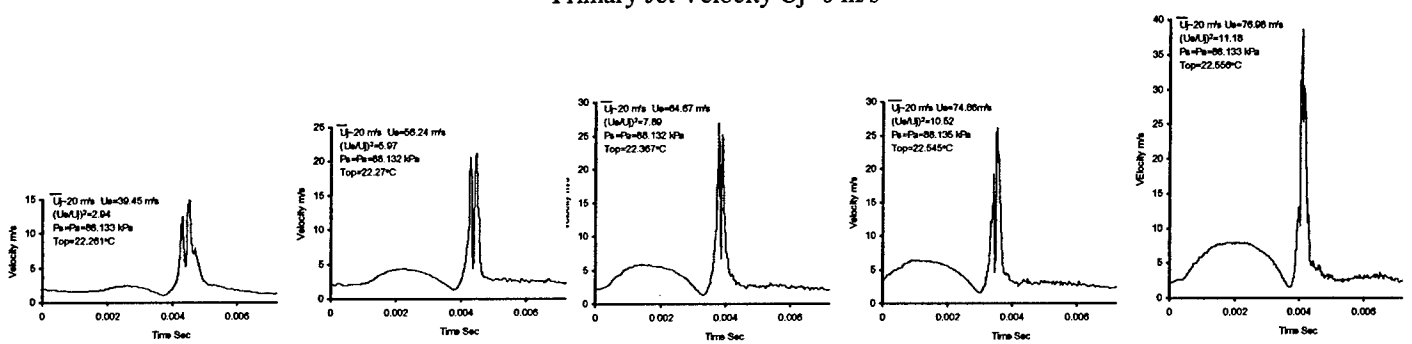

$(Ue/Uj)^2$=2.031 5.625 W | $(Ue/Uj)^2$=3.85 20.805 W | $(Ue/Uj)^2$=5.79 47.912 W | $(Ue/Uj)^2$=8.49 104.72 W | $(Ue/Uj)^2$=10.36 157.62 W

Primary Jet Average Velocity ~ 20 m/s Centreline Velocity 27.18 m/s

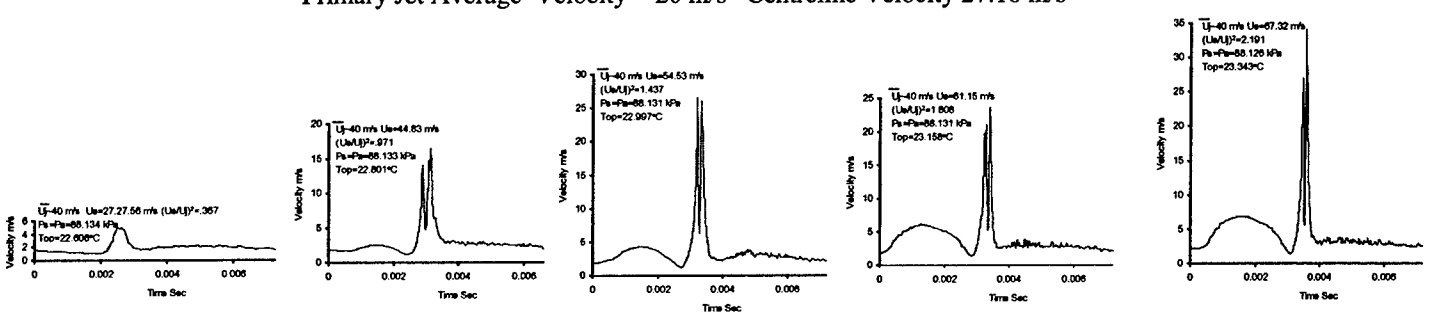

$(Ue/Uj)^2$=0.442 5.55 W | $(Ue/Uj)^2$=0.976 21.533 W | $(Ue/Uj)^2$=1.574 48.805 W | $(Ue/Uj)^2$=2.465 105.09 W | $(Ue/Uj)^2$=3.137 158.73 W

Primary Jet Average Velocity ~40 m/s Centreline Velocity 47.71 m/s

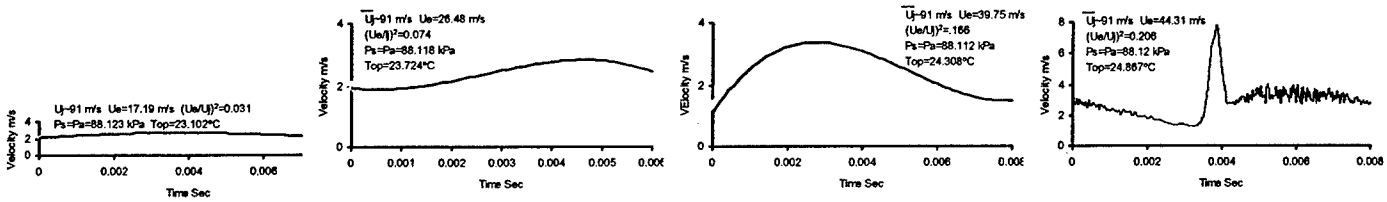

$(Ue/Uj)^2$=.0232 5.55 W | $(Ue/Uj)^2$=.0546 20.88 W | $(Ue/Uj)^2$=.166 100.68 W | (Ue/Uj)2=.2007 157.25 W

Primary Jet Average Velocity ~91 m/s Centreline Velocity=105.63 m/s

Fig. 3 Trace of Vortices at 0,20,40 and 91 m/s Primary Jet Velocity at Increasing Power to the Loudspeaker.

The windows of the test section were open so that the pressure in the test section was atmospheric. Pulsing an air jet appears to cause two modes of instability [12,13]. In the first mode when the jet flow is laminar, excitation develops in the thin laminar boundary layer before forming a train of traveling toroidal vortices. When the jet flow is faster and turbulent, the boundary layer cannot sustain oscillations, but waves form in the jet. This behavior is shown in figure 3 at the higher $\overline{Uj}$ of 91 m/s. As the strength of excitation is increased, these waves curl up and again form a train of traveling toroidal vortices. At stronger excitations the toroidal vortices become wavy in the circumferential direction and cease to be circular.

As the input power to the speaker is increased, Ue increases and the strength of the vortex increases. This is indicated by the increase in velocity on either side of the vortex core. As the primary velocity $\overline{Uj}$ increases Ue appears to remain the same, but the ratio (Ue/Uj) decreases. Vortex strength, a function of this ratio decreases and finally at 91 m/s the presence of a vortex is hardly noticeable until high power is input to the speaker. Experiments showed that the corresponding P.E. and P.E.R. also behaved similar to the vortex strength and proportional to $(Ue/Uj)^2$. Thus for a 5.13 mm dia. nozzle and a 40° Cone and 22.7mm dia. mixing tube at 150W power input, at 20 m/s primary velocity $(Ue/Uj)^2$ was 11.14, P.E. was 15.25 and P.E.R. was 3.97, whereas at 91 m/s primary velocity, $(Ue/Uj)^2$ was 0.215, P.E. was 4.75 and P.E.R. was 1.196.

The vortices shown in figure 3 cause a velocity profile across the entrance cone as shown in figure 4. It shows the velocity profile across the 40° entrance cone with a 22.7mm dia. cylindrical mixing tube, 1-dia. downstream of a 5.13mm dia. primary nozzle at a primary jet velocity of 38.634 m/s driven at 175 Hz and electric power input to the speaker of 100W. The plots are at 0.1633 ms intervals, starting when the current input to speaker was at a minimum. The 35 plots represent changes in the profile as the speaker undergoes one complete cycle. The solid line represents the pulsed jet and it is apparent that the area under it is always greater than the area under the dotted line of the steady jet. Numerical integration of these curves over the appropriate area results in figure 26.

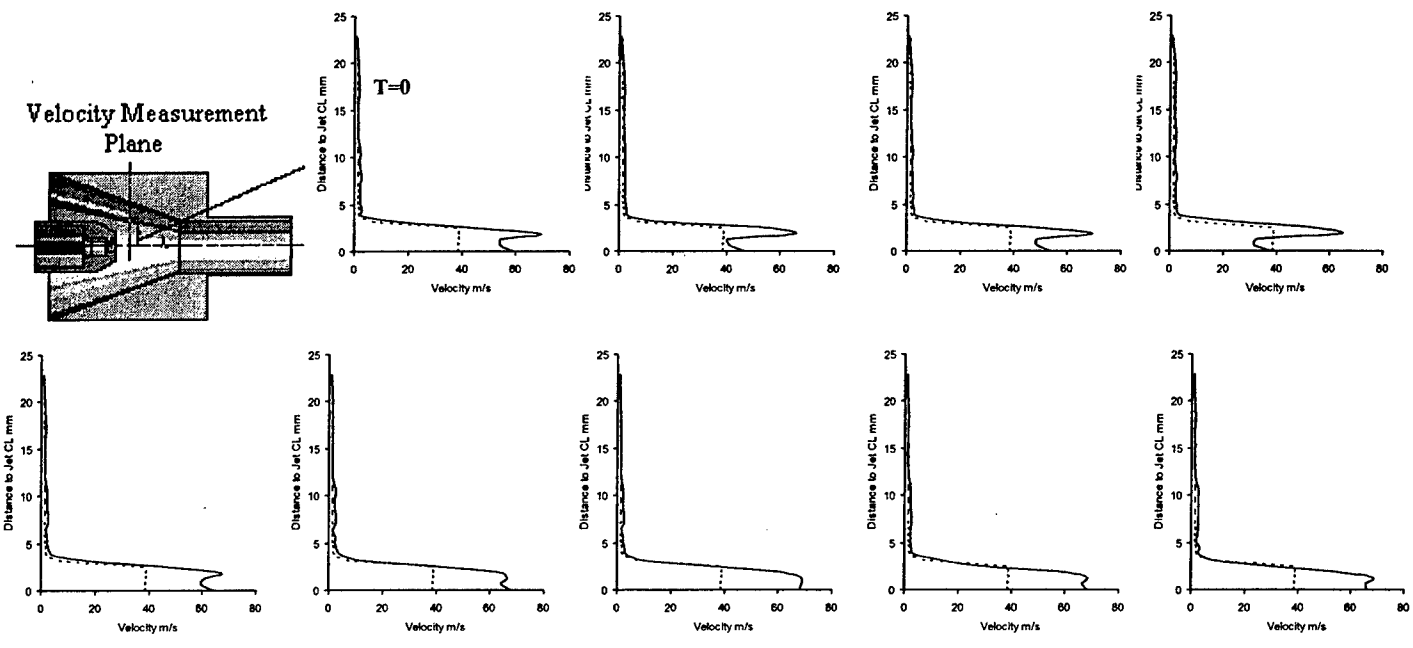

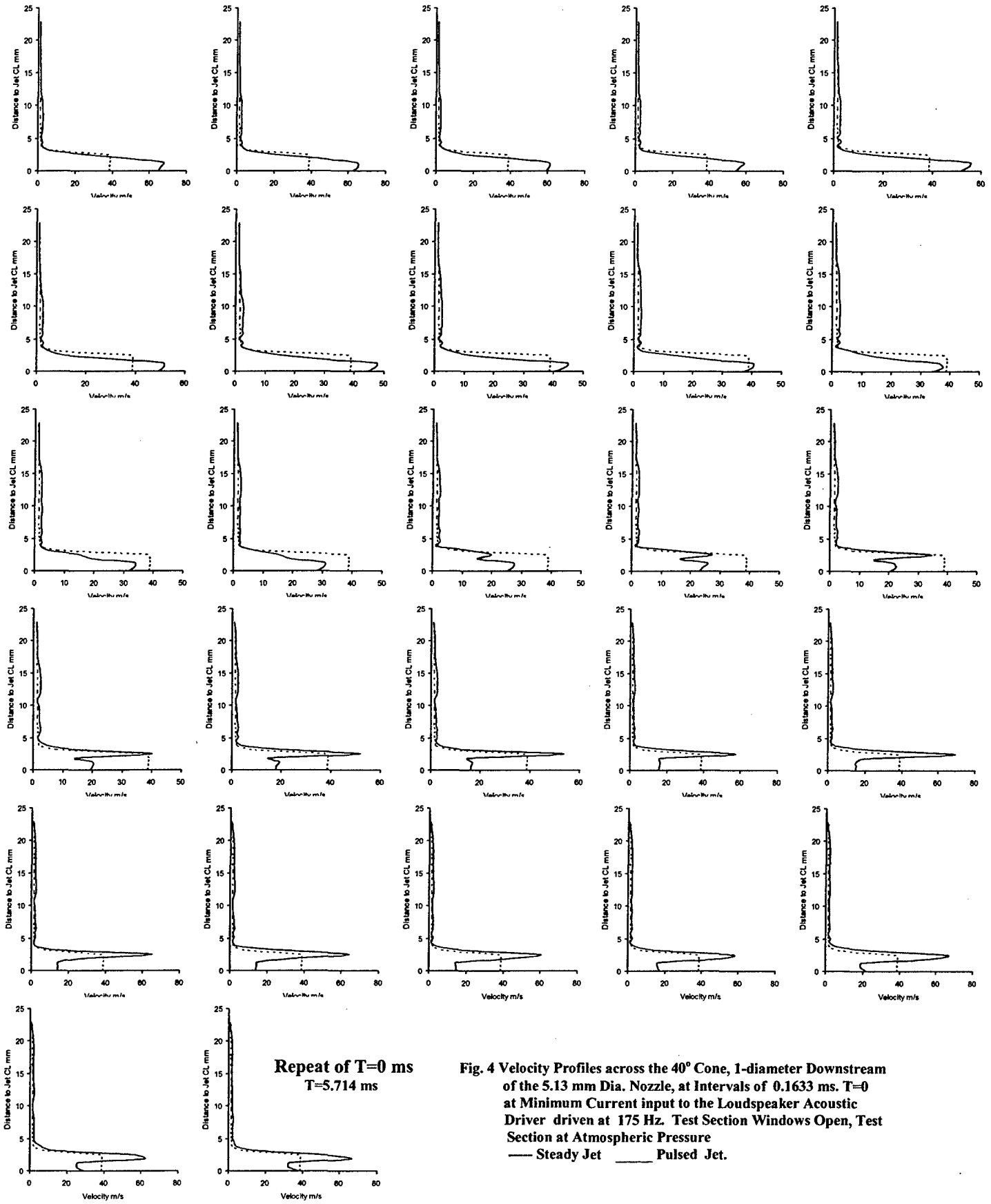

Fig. 4 Velocity Profiles across the 40° Cone, 1-diameter Downstream of the 5.13 mm Dia. Nozzle, at Intervals of 0.1633 ms. T=0 at Minimum Current input to the Loudspeaker Acoustic Driver driven at 175 Hz. Test Section Windows Open, Test Section at Atmospheric Pressure
—— Steady Jet ____ Pulsed Jet.

Jet flow entrainment is a boundary phenomenon. The physics of enhancement of entrainment due to pulsation appears to be caused by the high velocity at the boundary of the jet when pulsed. This velocity is independent of the average velocity of the jet and depends only on the pulsation strength of the vortex generated at the wall of the nozzle as shown in figure 3. The maximum velocity at the jet boundary occurs when the velocity at the centre-line of the jet is at a minimum as seen in figure 4. A steady jet also entrains air. This entrainment is presumably a boundary phenomenon and it has been shown that [19], for a steady jet,

$$Ms = \left[Ce \frac{Lm}{Dj} \left(\frac{\rho_s}{\rho_j} \right)^{1/2} - 1 \right] Mp, \qquad (1)$$

the value of Ce varying in the region of Lm<15 Dj and increasing to a fully developed value of 0.32.

Thus Ms is proportional to Mp and consequently to $\overline{Uj}$. Now if a velocity greater than $\overline{Uj}$ is generated at the boundary of the jet by pulsing, then presumably Ms will increase as if Mp has been increased. Energy considerations in appendix 2 indicate that as shown in figure 5 Ms is proportional to $(\overline{Uj}^2+1.5Ue^2)^{1/2}$.

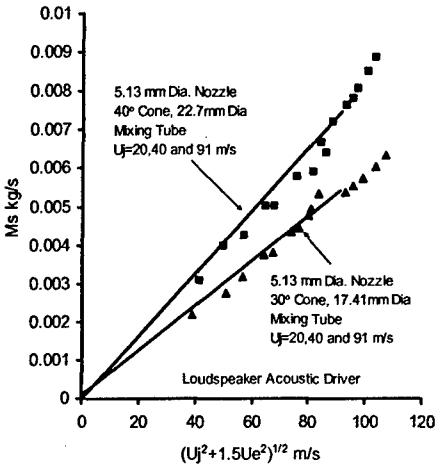

Fig. 5 Comparison of Steady and Pulsed Jets.

The two solid lines are for steady jets at approximately 0, 20,40 and 91 m/s for the 40° cone with 22.7 mm dia. cylindrical tube and a 30° cone with 17.41 mm dia. cylindrical mixing tubes respectively. The points plotted correspond to the jets pulsed at a range of Ue's and show good agreement with the steady flow. This suggests that pulsation is more effective in entraining ambient air than the steady jet. This may be due to the vortex action which causes the high velocity at the jet boundary. The vortex rotation may also cause ambient air to be swept into the jet.

Experimental work

Figure 6 shows the experimental set up with either the loudspeaker acoustic driver or the disc R.V.P.. A detachable nozzle meter was used when the R.V.P. was attached. This figure is taken from previous work and was also used in crossflow experiments [3,4]. The ejector was similar to the one chosen for computational fluid dynamics (CFD) investigation. The previous work had a 10.03mm primary nozzle diameter Dj , but a 5.13mm dia. nozzle was used in these experiments as the 17.41mm dia. cylindrical mixing tube appeared to be constraining the flow. The primary nozzle was designed as per British Standard 1042 with sharp edged exit. Both primary and secondary air supplies were from the laboratory air supply.

When the loudspeaker acoustic driver was used to pulse the primary flow, primary massflow rate Mp and secondary massflow rate Ms were both measured by orificemeters in the respective air lines. The two orificemeters were designed according to the requirements laid down in British Standard 1042. To avoid pulsations affecting the orificemeter measurements, the primary line had a choked nozzle upstream and a large volume downstream of the orificemeter. The large volume of the entrance of the secondary flow into the test section, muffled any pulsations reaching the secondary orificemeter. There was also provision made to measure such parameters as the primary flow stagnation temperature Top, static pressure Pp. During the experiment secondary flow was adjusted so that the static pressure in the test section Ps was atmospheric. The stagnation pressure Pos and temperature Tos in the test section was also measured. The static pressure P_t just downstream of the cylindrical mixing tube was also noted. Figure 7 is from figure 6 and gives the locations for the measurement of these properties.

Tests were conducted for the 5.13 mm dia. standard sharp edged nozzle with a concentric mixing tube consisting of 21° cone, 30° cone, 40° cone and a ssimple bellmouth entrance and a 17.41 mmdia. tube of length equal to 153.2 mm. Originally this length was selected so that the distance from nozzle exit plane to mixing tube exit would be 10 times the diameter of the cylindrical portion of the mixing tube. A standard Venturi with a 21° contraction cone, a 17.41 mm dia. throat and a 12° diffuser was also tested. For all these configurations S the spacing between the nozzle exit plane and the throat of the mixing tube was varied from 11.17 mm to 76.72 mm.

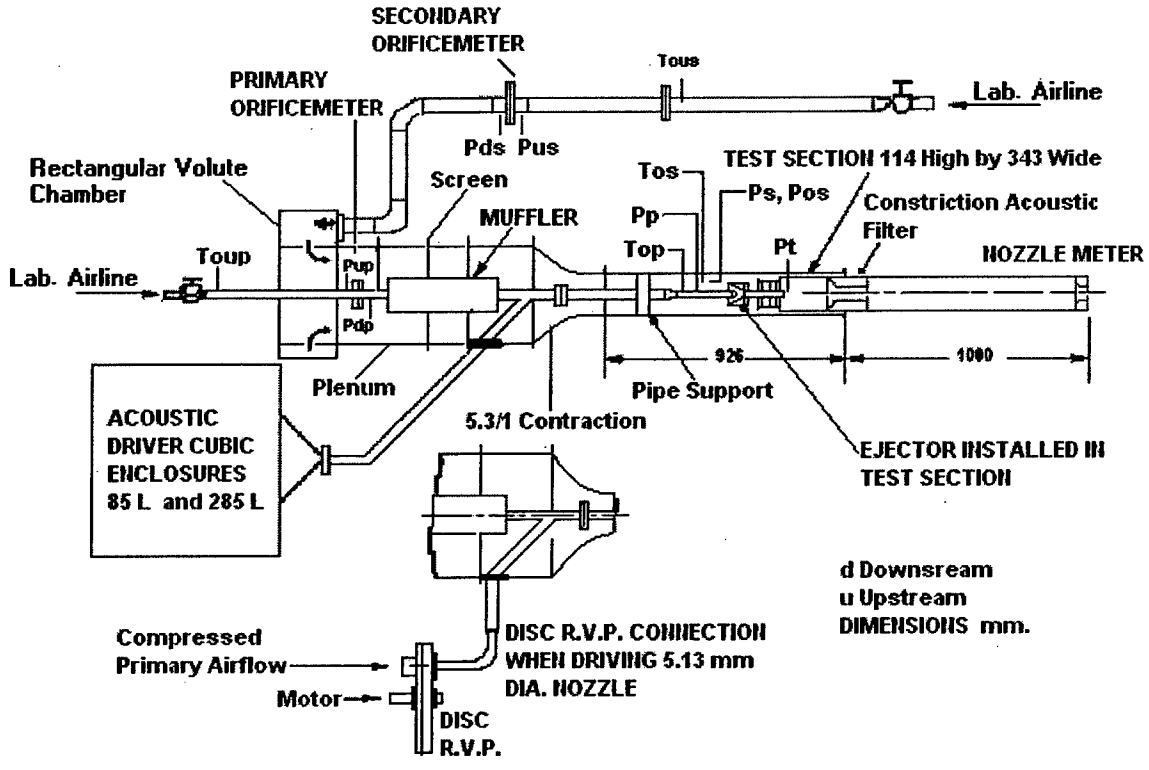

Fig. 6 Pulsed-Ejector Test Rig With Compressed Air Feed, With Nozzle Meter Installed When Disc R.V.P. Tested.

Results from these tests done with the loudspeaker acoustic driver indicated the 17.41mm dia. cylindrical mixing tube was perhaps constraining the flow and limiting the ejector performance. To investigate this, tests were carried out with a 22.7mm dia. cylindrical portion of the mixing tube. 22.7 mm dia. was selected as it is more than 4 times the nozzle diameter. The cylindrical tube with a 40° cone entrance and a circular plate with a rounded entrance into this tube were tested.. There appeared to be no change in the performance. The tube was therefore tested by itself.

A dimensionless mass flow rate parameter may be formed by division of the flow numbers $Ms\sqrt{RTos}/PosDm^2$ and, $Mp\sqrt{RTop}/\overline{Poj}Dj^2$ where R is the specific gas constant for air and $\overline{Poj}$ is the jet flow average stagnation pressure.

Pumping Effectiveness of the ejector

$$P.E.D.=\frac{Ms}{Mp}\frac{\overline{Poj}}{Pos}\sqrt{\frac{Tos}{Top}}\frac{Dj^2}{Dm^2} \qquad (2)$$

For specific Dj and Dm, the ratio (Dj/Dm)2 is a constant and can be dropped to give a less general dimensionless pumping effectiveness parameter:

$$P.E. = \frac{Ms}{Mp}\frac{\overline{Poj}}{Pos}\sqrt{\frac{Tos}{Top}} \qquad (3)$$

To compare pumping effectiveness of pulsed(WD) and steady (ND) jets Pumping Effectiveness Ratio P.E.R. is defined:

$$P.E.R.=\frac{\left[\frac{Ms}{Mp}\frac{\overline{Poj}}{Pos}\sqrt{\frac{Tos}{Top}}\right]_{WD}}{\left[\frac{Ms}{Mp}\frac{\overline{Poj}}{Pos}\sqrt{\frac{Tos}{Top}}\right]_{ND}} \qquad (4)$$

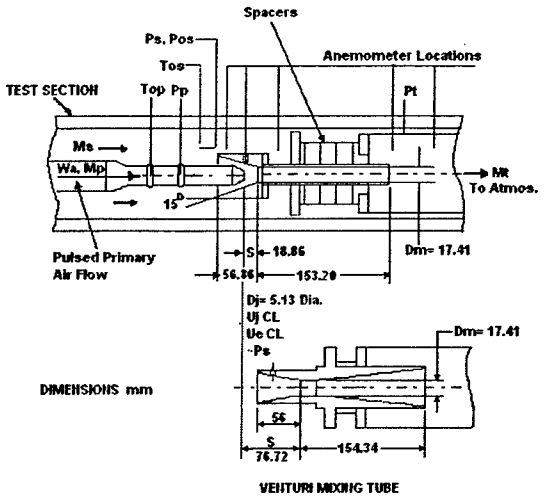

Fig. 7 Pulsed Air Ejector Installed in Rig Test Section,DrivenbyLoudspeakerand 5.13 mm Dia. Nozzle, 30o Cone-Cylindrical Mixing Tube and Venturi Mixing Tube Selections.

P.E.R. is independent of the diameter size normalizing and represents a normalized Ms(WD)/Ms(ND). Jet stagnation pressure $\overline{Poj}$ is corrected for pulsations by P.E.R. is independent of the diameter size normalizing the use of equation

$$\overline{Poj} = Pj + \frac{\rho j}{2}\left[\overline{Uj^2} + \frac{Ue^2}{2}\right] \qquad (5)$$

when the loudspeaker acoustic driver was used as its pulsing was sinusoidal. When an R.V.P. was used since the anemometer voltage
was available at each point of the pulse, compressible equations at the nozzle exit conditions were used to obtain both pulse velocities as well as the stagnation pressures to give these velocities.

The stagnation pressure was then averaged over the pulse to obtain $\overline{Poj}$.

It is shown in the appendix, $(Ue/Uj)^2CL$ is a measure of the energy in the jet flow. Also previous work [18] has shown that

$$\left(\frac{Ue}{Uj}\right)^2 = K\frac{Wa}{\rho j Dj^2 Uj^3} \qquad (6)$$

for constant frequency, where Wa is the acoustic power input to the jet, ρ_j is the jet density at nozzle exit and K is a constant dependent on Reynolds number Re. That is, $(Ue/Uj)^2$ and $(Ue/Uj)^2CL$ are proportional to the acoustic power that the pulsator imparts to the jet flow. For this reason P.E. and P.E.R. are plotted against $(Ue/Uj)^2_{CL}$.

The general layout of the pulsed ejector test rig in figure 4 also shows details of the rotary valve pulsator mounting. The details of the method used for calculating P.E. and P.E.R. in this case are shown in the flow chart in appendix3. Initially the hot film anemometer was calibrated with the TSI Model 1125 calibrator. Using the nozzle upstream pressure and the exit atmospheric pressure, compressible flow equations gave density multiplied by velocity at the prescribed distance downstream of the nozzle. This was calibrated against Voltage.

During the entrainment measurement tests Mp was determined by placing the calibrated hot film anemometer probe at the centre of the primary nozzle, one nozzle diameter downstream. The pulsed flow time-voltage trace was taken on a Bruel Kjer Dual Channel analyzer and the values read off the analyzer. By employing compressible flow equations for the measured nozzle exit conditions and using hot film, anemometer calibration the time-voltage values were converted to time-(density x velocity), which was then integrated and averaged. Multiplying this by the area of the nozzle resulted in primary massflow rate measured at the centerline of the nozzle. This was then corrected to the average masflow. This was done as follows. During the tests with the loudspeaker acoustic driver, the centerline velocity was measured by the hot film anemometer for steady jet case. For this test the average massflow rate was also measured using the orificemeter.From these a scaling factor between the average and the centerline massflow rates was established and used to correct the centerline massflow rate. An integrated average centre line jet velocity was also obtained in the same manner. Later, when LabView computer software became available, the time-voltage values of the pulse was read by its use and stored into a disc.

The second method for measuring primary flow rate Mp was to employ a nozzle meter shown in figure 6. This measured the total flow rate M_T = (Mp+Ms) and since Ms was measured by the orificemeter Mp could be

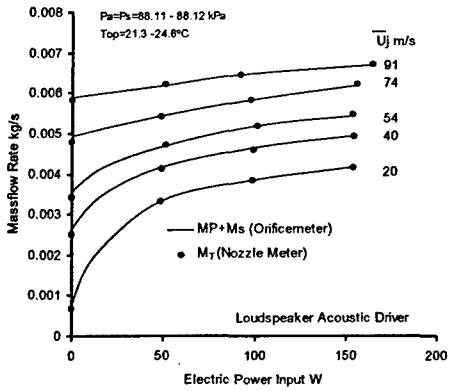

Fig. 8 Comparison Between (MP+MS) Measured by Orificemeters and MT by Nozzle Meter.

found. The nozzle was 19.16 mm dia. measuring nozzle designed according to the British Standard 1042. It was checked against the two orificemeters by running tests with the loudspeaker acoustic driver.

Figure 8 shows the correspondence between (Mp+Ms) measured by orificemeters and M_T measured by the Nozzle meter at various electrical input power to the loudspeaker acoustic driver for primary flow velocities of 20,40,54,74 and 91 m/s.

The plot shows there is an excellent agreement inspite of residual pulsations present in the flow upstream of the measuring Nozzlemeter.

Other aspects of tests conducted with the R.V.P. were same as for the loudspeaker acoustic driver.A few tests were also Performed with the dumbbell, piston-cylinder pulsators. These tests were similar to the R.V.P. tests.

Since $(Ue/Uj)^2CL$ is the parameter against which P.E. and P.E.R. are plotted experimental determination of Ue is detailed in figure 13 of reference 14.

Pulsators

It is evident that $(Ue/Uj)^2CL$ is a direct function of the acoustic power input to the jet, pulsators which can impose strong velocity pulsations have to be utilized. Pulsing the primary flow and the means to do so is integral to the project. This section is devoted to pulsators.

a) Loudspeaker Acoustic Drivers

Most of the experiments were carried out using loudspeaker acoustic drivers consisting of a 8 ohm H2226 600W JBL speakers, with the recommended enclosures of volume 85 and 285L. The pulse obtained was sinusoidal and the maximum power at which these speakers were driven continuously was 150W. This type of pulsators are very convenient as both the frequency as well as the amplitude of pulsation can easily be controlled. At the same time once a loudspeaker is attached to the system, the integral system has a resonant frequency at which the speaker performs best. Maximum pulsations are obtained only at this frequency. Even though changing frequencies is easy, the loudspeaker is best used at this resonant frequency. The system resonant frequency in these experiments was 127 Hz for the small enclosure and 131 Hz for the large enclosure. More powerful speakers with metal bellows are becoming available which may lead to their use in practical applications.

b) Rotor Pulsator Valve (R.V.P.)

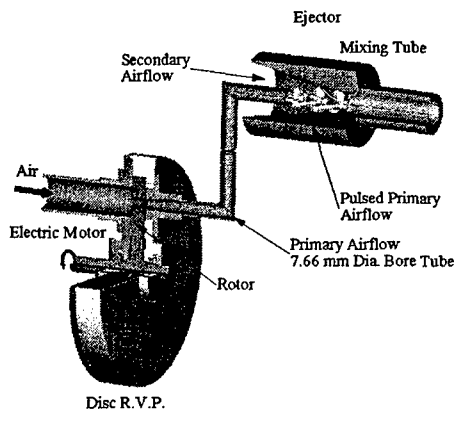

Fig. 9 Disc Rotor Valve Pulsator(R.V.P.) Tube Pulsed Ejector.

In the final version as shown in figure 9, it consisted of a 7.6mm thick disc rotaing inside an outer casing with slide fit clearances. The disc had 3-6.35mm dia. holes and the casing had 6.35 holes which were in line. Air was fed from the laboratory supply and when one of holes in the disc lined with the casing holes, a pulse would be generated. The pipe through which this pulse traveled into the test section had to be very short to allow air to empty. Otherwise the lower velocity of the pulse was high.

Some tests were conducted with this pulsator and representative pulse shapes are given in figure 9 with the corresponding test conditions.

Figure 10a shows the effect of increasing the flow rate through the pulsator leading to reflected waves which tend to increase the minimum velocity in the pulse. These two cases give surprisingly good values of P.E.R.. This is attributed to the sharp shape of the velocity time pulse.

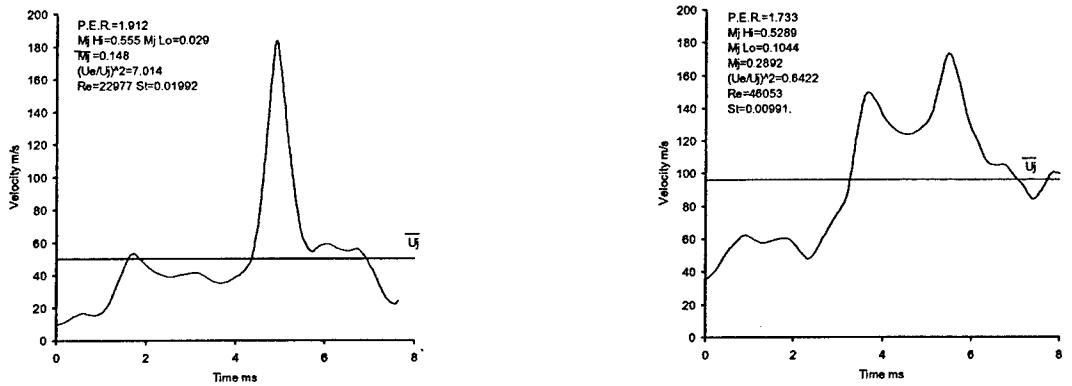

Fig. 10a Effect of Increasing flow rate through the Pulsator.

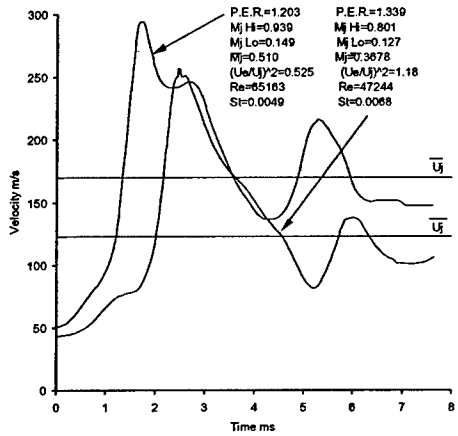

Fig. 10b Velocity Pulse Shape At Increasing Flow Mach Number.

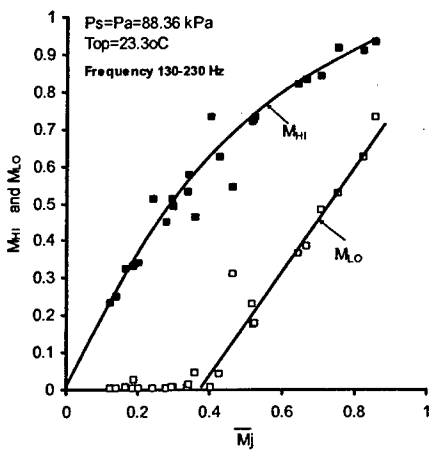

Fig. 10c Pulse High and Low Mach Numbers with Increasing Flow.

Since practical primary Mach numbers are of interest, increasing the Mach number close to 0.5 was attempted. Such experiments generally lead to P.E.R. being very low. Thus when the average flow Mach number is 0.37 and 0.51 as in figure 9b, P.E.R. drops to 1.34 and 1.20. More results are given for the R.V.P. in the results section.

There are two disadvantages to the R.V.P. namely 1) average flow Mach number and the highest pulse velocity are interrelated and since the flow has to pass through a hole whose area changes from zero to maximum, back to zero, the flow is extremely turbulent. This large scale turbulence in the flow appears to submerge any vortices that may be present. It was not possible to obtain the M-shaped velocity trace. The losses in the flow are very high and 2) mechanical problem at higher flows, the pressure on the rotor face made it impossible to keep the rotational speed constant if the clearances between the rotor and the casing is tight. Increasing the clearance causes leakage past the rotor, thereby allowing high pressure air past the rotor into the exit tubing and raising the minimum velocity of the pulse. This is evident on Figure 10c, a plot of average flow Mach number against the high and the low Mach Numbers encountered on the pulse. Beyond about 0.4 Mach, the pulsation strength is severely compromised by the leakge past the rotor.

c) Dumbbell Pulsator

The working of this dumbbell shape of free piston pulsator is self evident The piston travels back and forth opening and cutting off the flow to the two outlets of air as shown in figure 11, thereby creating a pulsed flow in the two outlet tubes. It was not possible to achieve more than 50 Hz with the pulsator built. It is possible that smaller

pulsators would give higher frequencies, but the turbulence created by the moving piston dominated any vortices generated. The losses in the flow were very high and the maximum pulse Mach number obtained was 0.8.

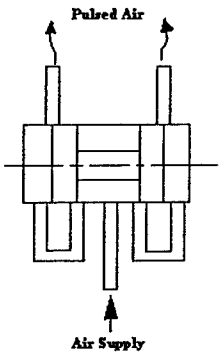

Fig. 11 Dumbbell Pulsator.

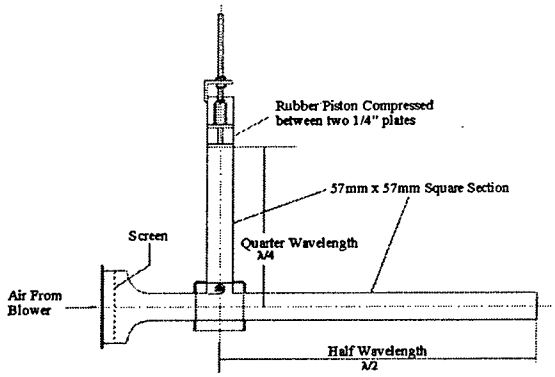

Fig. 12 Aero-Acoustic Pulsator.

d) Aero-Acoustic Pulsator

This is a very attractive idea for a pulsator as it promises to have low losses. As shown in figure 12, a vortex is generated at the edge of the T-junction which travels up the stem and reflects back to in time to strengthen the next vortex generated, if the lengths of the pipes are made right. If the end of the horizontal pipe is open, then its length shoud be half the wavelength and the vertical pipe should be quarter the wavelength, for a designated frequency. Tests in other labs have indicated that a value of $(Ue/Uj)^2$ of one can be obtained for a Strouhal number of 0.3.

Unfortunately, all attempts to duplicate these numbers failed.A pulsator built with 57 mm square tubing, designed to give 250 Hz made some noise which was not a pure tone. Hot film anemometer placed in front of the exit showed no pulsations.Many of these devices were built, with round tubes, small and large square tubes etc. but none showed any promise.

e) Tube Pulsator

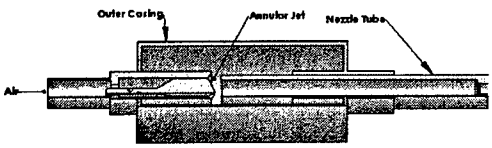

Fig. 13 Tube Pulsator.

The idea for this pulsator also originated at a late stage of this project which is unfortunate as it has shown the most promise.

The air supply is accelerated through an annular space, 22.53mm outer dia. and 21.92mm inner dia. as shown in figure 13 . This annular area is flared at the end to an included angle of 120°, to facilitate flip-flopping. The resulting annular jet impinges on a 25.4mm outer dia. and 19.05mm inner dia. tube. This tube is rounded to its thickness at this end and has a nozzle at the other end. An outer casing encloses the tubes and the jet.

Theoretically, this pulsator works on the principle of a flue tube . When the pulsing starts, if the flow of air is through the nozzle tube, then the annular jet entrains air from the outer casing and reduces the pressure there. This causes the annular jet to flip over to the outer casing. The jet is flipped back into the tube by the pressure build up in the outer casing as well as by the pressure reduction in the tube due to entrainment.

Tests were carried out to investigate the velocity variation in the pulse so produced. The pulsator requires holes in the outer casing to give good pulsation. Thus figure 14 shows the velocity variation at approximately 2540 Hz for 1,2,3 and 4 6.35mm dia. holes in the casing. The highest velocity obtained on the pulse for upto 3 holes was about 165 m/s. The lower velocity for these cases decreased with the number of holes, the lowest for 3 holes. When the number of holes was increased to 4, the highest velocity went down to about 120 m/s. The lowest was about 40 m/s. The pulse strength decresed.

The number of holes needed appears to depend on the nozzle tube attached. The greater the friction it offers to the flow the fewer the holes required. This is as expected as, if friction is high then the pressure at the entrance to the tube will also be high. The pressure in the outer casing has to be high to push the jet back into the tube.

Also the possibility of attaching similar tube pulsators using the air from these holes needs to be explored. The strongest pulse was obtained for 2 and 3 holes, the highest velocity in the pulse being 160 to 170 m/s and the lowest about 60 to 65 m/s. Bench tests have also indicated the presence of vortices where expected showing similar behavior to the loudspeaker driver as in figure 3. The strongest pulse was obtained for 2 and 3 holes, the highest

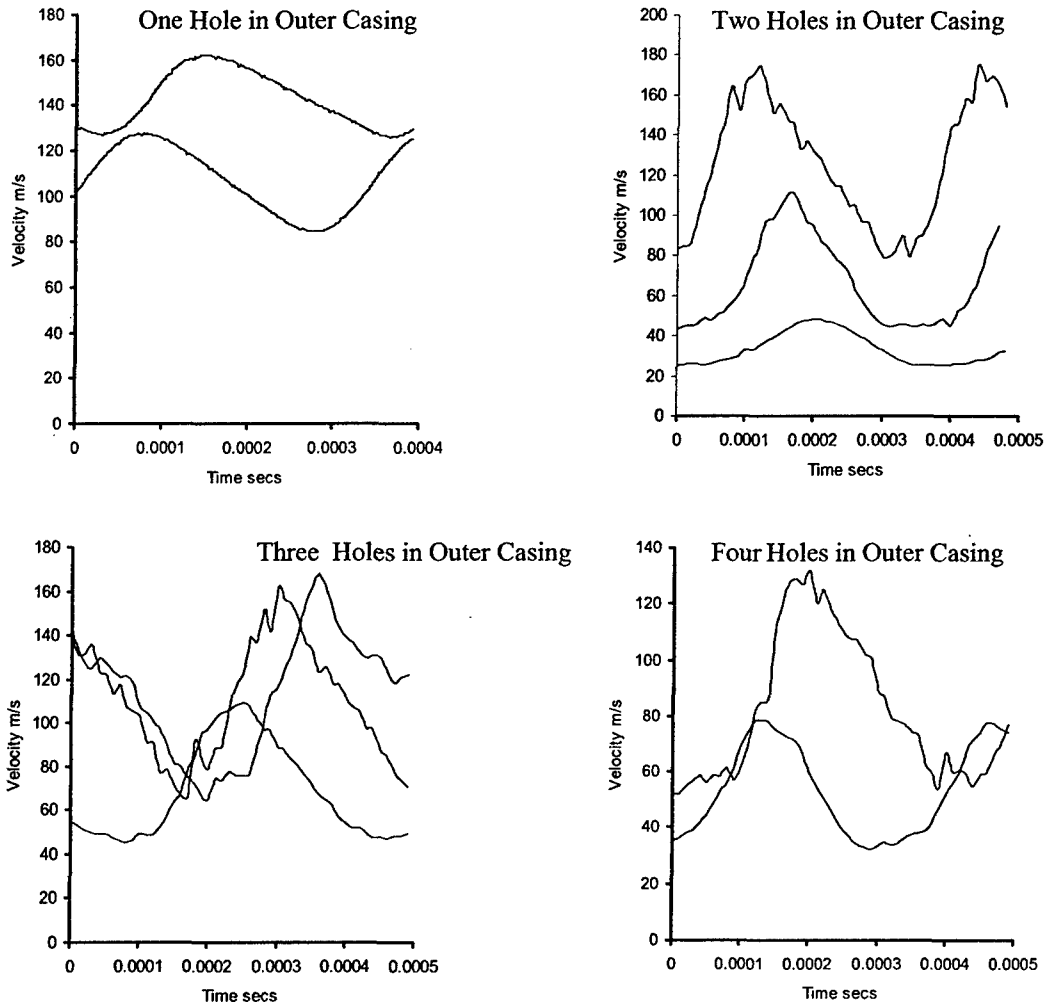

Fig. 14 Measured Tube Pulsator Velocity Pulsations.

f) General Electric Synthetic jet

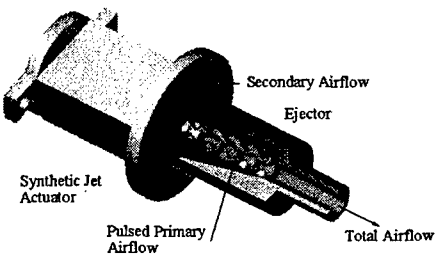

Fig. 15 Synthetic Jet Actuator Ejector

No mechanical details are known for this pulsator which gives pulsation only. There is no primary flow as such. It is very attractive for this reason as no air is needed for primary jet flow. The highest velocity was obtained at 820 Hz and was 111 m/s and the minimum for this pulse was 34 m/s. There was some electrical problem with the pulsator at the time of testing as the design maximum velocity was claimed to be very much higher. Results are given for this pulsator and compared to tests where there was a primary flow in figure 11 of reference 14.

g) Piston-Cylinder

A lawn mower engine piston-cylinder combination driven by an electric motor was tried as a pulsator. It was attached to by a T-connection to the primary flow air supply line and tubed directly into the test section as in the case of the R.V.P.. The maximum frequency obtained was about 45 Hz. The piston was 31.75 mm Dia. and had a stroke of 25.4 mm. Beyond 45 Hz which corresponds to 2700 rpm, the vibrations became too severe. This was the highest frequency tested. The results obtained were as good as those for te R.V.P..

Experimental Results for the Ejector Driven by Loudspeaker and Nozzle

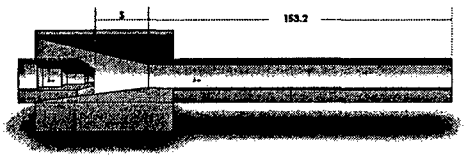

30° Cone Entrance 17.41mm dia. Cylindrical Tube

Figure 15 shows the various geometries of mixing tubes tested. The cylindrical portion of the mixing tubes were 17.41 mm dia..In the precursor work [1] the distance from the nozzle exit to the mixing tube exit was fixed at10 diameters of the cylindrical portion of the mixing tube. The throat spacing S was 1 diameter, making the length of the cylindrical portion of the mixing tube 153.2 mm. The entrance cones were 21°, 30° and 40°.

The other mixing tubes tested were a bellmouth rounded to 10 mm dia. and a standard Venturi with a 21° contraction cone, a 17.41 mm dia. throat and a 12° diffuser . The exit was 46 mm dia.

21° Cone Entrance 17.41mm Dia. Cylindrical Tube.

Bellmouth with 17.41mm Dia. Cylindrical Tube.

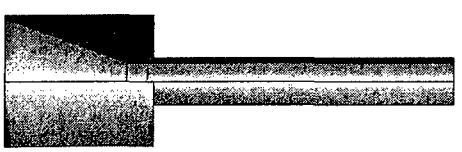

40° Cone Entrance 17.41mm Dia. Cylindrical Tube.

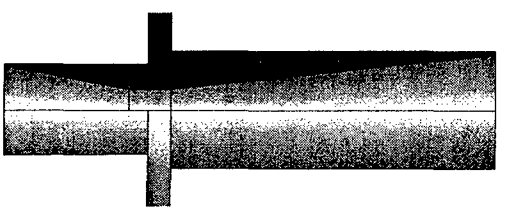

Standard Venturi 21° contraction 17.41mm Dia. Throat, 12° Diffuser.

Fig. 16 Geometry of the Mixing Tubes Tested.

The results obtained from tests conducted on these mixing tube geometries for electric power input of 0,5,20,50,100 and 150 W, for various throat spacings ranging from 11.17 mm to 76.72 mm are given in reference 14, a paper presented at the 2nd AIAA Flow Control Conference, held between 28 June and 1 July 2004,in Portland, Oregon. A table in appendix 2 lists the nozzle and mixing tube geometry for the tests conducted.

Two inferences that can be drawn from the results given are that apart from what appears to be a second order of magnitude change in P.E. due to Re and Strouhal number, the values of P.E. do not change very much for the different entry cones. It appears that the cylindrical portion of the mixing tube is constraining the flow.

The only noticeable change is for the Venturi and that is presumably due to the pressure recovery in the diffuser. This lack of change in P.E. values for the three cones indicates there is little effect on P.E. due to the entrance geometry, if the downstream cylindrical tube is constraining the the flow.

A simple experiment was carried out during which, the stagnation pressure Pos in the test section was measured when a given flow rate Ms exiting out of the test section to atmosphere , through the Venturi mixing tube

and the 21° Cone with 17.41mm Dia. cylindrical mixing tube. Since Ms is a function of velocity, a plot of Ms versus the square root of the difference in pressure $(Pos-Pa)^{1/2}$ was made and is shown in figure 17.

It is evident that the Venturi only requires about half the pressure for the same flow rate to exit. It is also to be noted that P.E. for the Venturi is twice as much as for the cone entrances. There is a slight decrease in pressure as throat spacing S increases for the Venturi. The effect is opposite for the 21° Cone entrance, pressure increasing as S increased As expected P.E. behaved in the opposite manner in that it increased with increase in S for the Venturi and decreased for the cone when S increased.

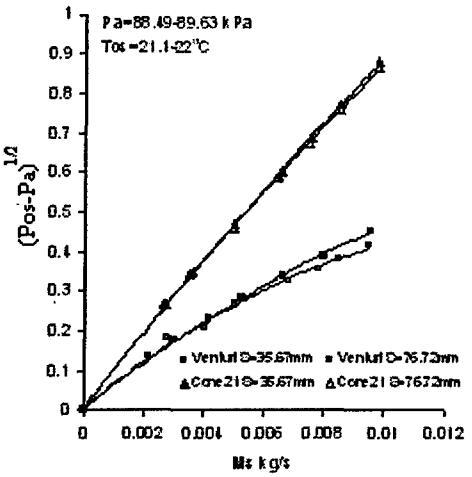

Fig. 17 Square Root of Test Section Stagnation Pressure over Exit Atmospheric Pressure to Cause A Mass Flow Rate of Ms

It appears the performance of mixing tubes can be easily compared by the simple expedient of finding out the stagnation pressure in the test section needed to cause a given flow rate to exit through the mixing tube.

To determine if the 17.41 mm dia. cylindrical tube was constraining the flow, three other mixing tube geometries were tested. The details of these geometries are given in figure 18. The important change from the previous mixing tubes is that the cylindrical tubes in these were 22.7 mm dia.. This dimension was decided upon after examining figure 1, where the pulsed jet opens up to 4 times the diameter of the primary nozzle almost immediately downstream of the nozzle. The length was made 202 mm, approximately 9 times the diameter.

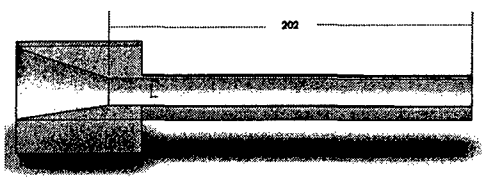

40° Entrance Cone, 22.7 mm Dia. Cylindrical Tube.

22.7 mm Dia. Cylindrical Tube.

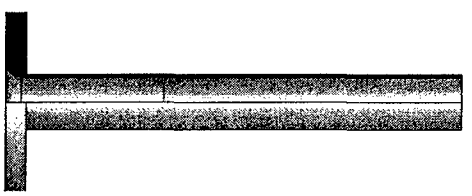

101.6 mm Dia. Plate Rounded to 7 mm. Radius at Entrance to the 22.7 mm Dia. Cylindrical Tube.

Fig. 18 Geometry of Bigger Diameter Mixing Tubes Tested.

Table in appendix 1lists the geometry of the nozzle and mixing tube for the various tests conducted with these mixing tubes. Figures 19and 20 give the results. It was found that the cone and the plate entrances gave virtually the same results, both approximately 27% better than the 17.41mm dia. cylindrical tube geometries for P.E. values and about the same maximum P.E.R. value greater than 4. As the entrances appeared to have no influence on the performance of the ejector, the 22.7mm dia. tube was tested by itself. It can be seen from the figures 19 and 20 that the tube by itself is slightly less efficient than the ejector with the cone and plate entrances, but is still more efficient than the 17.41mm dia. cylindrical tube ejectors.

In these tests also there is an improvement in the ejector performance, though not by much, as the primary jet Re gets greater than 11764. This trend is present in the P.E.R. plot as well unlike that for the 17.41 cylindrical tube ejectors. Maximum value of P.E.R. is still greater than 4.

The difference in behavior between the tube by itself and the mixing tubes with cone and plate entrances is more noticeable in figure 21, which shows the behavior of P.E. for the 22.7mm dia. ejectors with various entrance geometries as the throat spacing S changes. P.E. decreases significantly for the 40° cone and the plate at Uj=20 m/s.

The change is not as steep for the tube by itself. In fact P.E. appears to flatten out as S increases. For the two other Uj values plotted P.E. does not show the same decrease as S increases. As far as P.E.R. as seen in figure 22, the values are less for the tube compared to those for the 40° cone and the plate at Uj=20 m/s, but are equal at the other two primary velocities. P.E.R. increases slightly as S increases as it did in the case of the Venturi mixing tube.

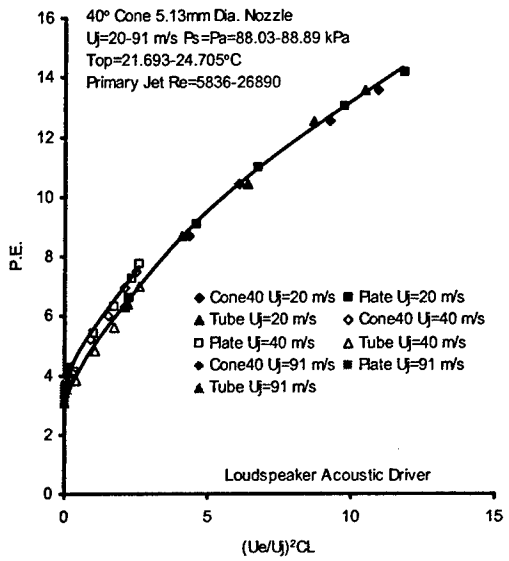

Fig. 19 Ejector Pumping Effectiveness P.E. Versus (Pulsation Strength)^{2}CL, Loudspeaker, 5.13mm Dia. Nozzle, 22.7 mm Dia. Cylindrical Mixing Tube, with Various Entrance Geometries. Throat Spacing S ~73mm.

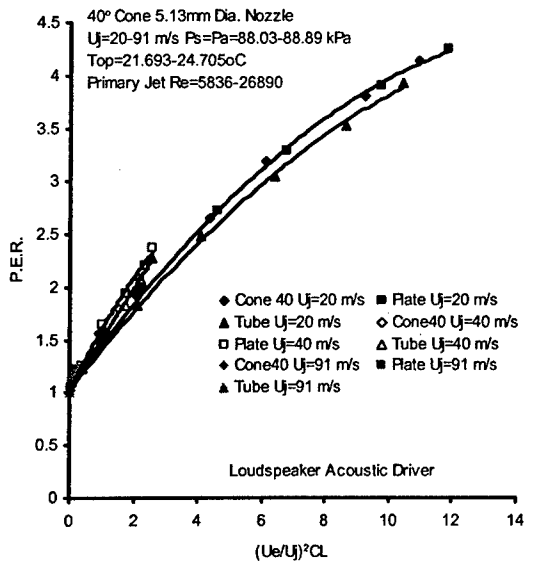

Fig. 20 Ejector Pumping Effectiveness Ratio P.E.R. Versus (Pulsation Strength)^{2}CL , Loudspeaker, 5.13mm Dia. Nozzle, 22.7mm Dia. Cylindrical Mixing Tube with Various Entrance Geometries, Throat Spacing 73mm.

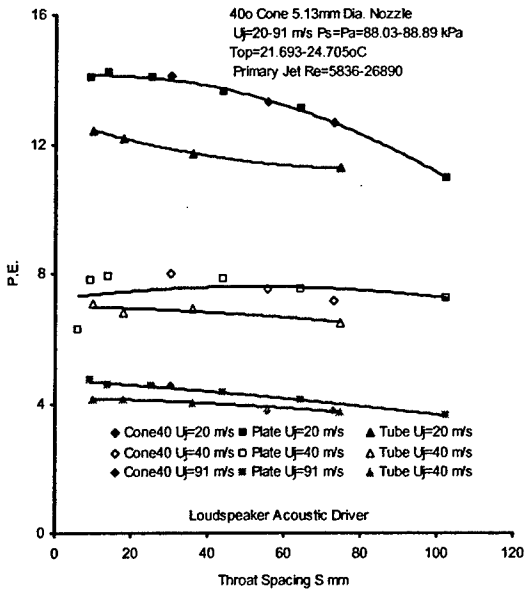

Fig. 21 Ejector Pumping Effectiveness P.E. Versus Throat Spacing S, Loudspeaker, 5.13mm Dia. Nozzle, 22.7 mm Dia. Cylindrical Mixing Tube, with Various Entrance Geometries. at 100W Electric Input Power to Speaker.

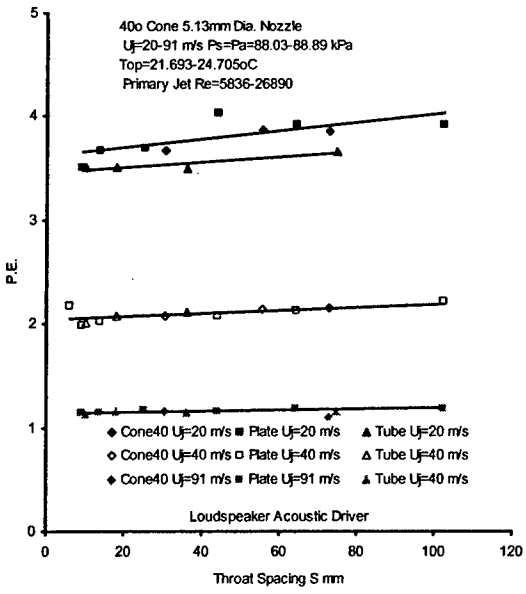

Fig. 22 Ejector Pumping Effectiveness Ratio P.E.R. Versus Throat Spacing S, Loudspeaker, 5.13mm Dia. Nozzle, 22.7mm Dia. Cylindrical Mixing Tube with Va rious Entrance Geometries, Throat Spacing 73mm.

From results for the 17.41 mm dia. cylindrical mixing tubes [14] and the results for the bigger 22.7 mm dia mixing tubes, it appears that the entrance geometries have little effect on the ejector performance. The downstream cylindrical portion is the important part.

Experimental Results for Ejector Driven by Disc Rotor Valve Pulsator (R.V.P.)

The table 3 in appendix 1 gives the geometry of the rotor valve pulsator, primary nozzle and the mixing tubes for the various tests conducted on the ejector with the R.V.P. driver. The frequencies are also given. The results from these tests are in reference 14.

Experimental determination of Ue,Uj and UjCL are detailed in figure 13 in reference 14. It is evident that a sharp pulse gives a better P.E.. High pulse Mach numbers could only be obtained when the holes in the rotor were large (19.05 mm Dia.). When the holes were smaller (^.35 mm Dia.) the losses were so great that high average or high maximum pulse numbers could not be obtained. Large holes on the other hand resulted in flat wide pulses which gave low $(Ue/Uj)^2CL$ values and low P.E. values. For small holes the pulses were much sharper but large scale turbulence made it impossible to detect any toroidal vortices thereby creating doubt as to their presence.

Experimental Results for Ejector Driven by Dumbbell Pulsator

Figure 22 gives the results for a 7.66 mm dia. bore tube in a Venturi mixing tube driven by a dumbbell pulsator. The Venturi mixing tube was the same on e used in the cone-17.41 mm dia. mixing tube experiments and had a 21° contraction cone, a 17.41 mm dia. throat and a 12° diffuser. The maximum pulse Mach number reached was 0.362. The frequency was restricted by the mass of the piston to 40 Hz. Again the losses restricted the maximum average flow Mach numbers as well as the maximum pulse Mach number. This pulsator was not pursued further. The results were similar to those obtained for the R.V.P. pulsator.

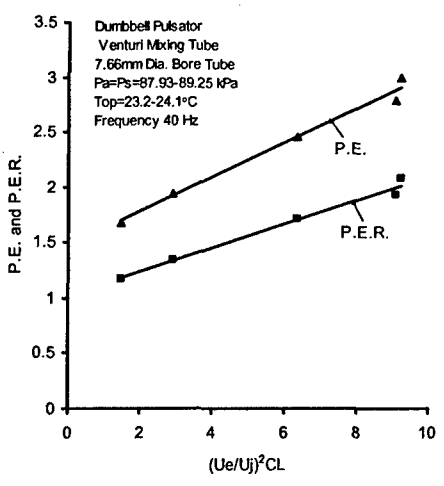

Fig. 23a Ejector Pumping Effectiveness P.E. andPumping Effectiveness Ratio P.E.R.Versus (Pulsation Strength)²CL Dumbbell Pulsator , 7.66 mm. Dia. Tube.

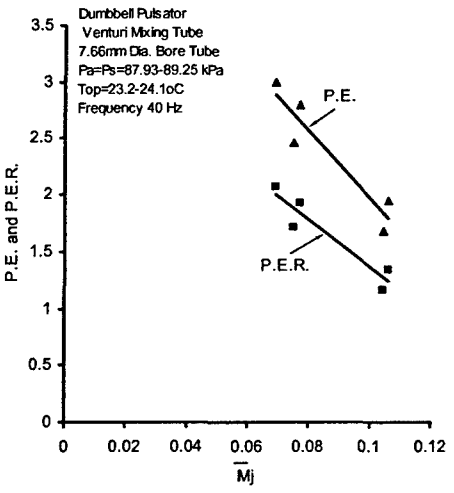

Fig. 23b Ejector Pumping Effectiveness P.E and Pumping Effectiveness Ratio P.E.R. Versus Average Jet Mach Number. Dumbbell Pulsator , 7.66 mm. Dia. Tube.

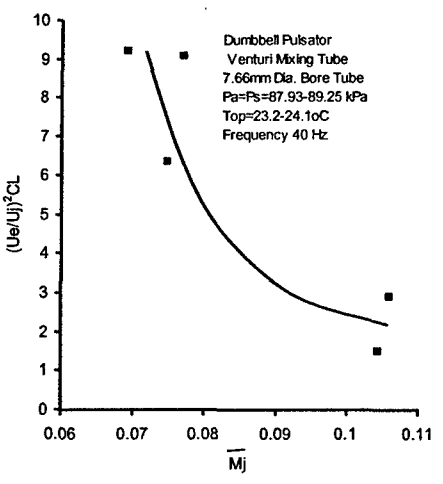

Fig. 23c (Pulsation Strength)²CL Versus Average Jet Mach Number. Dumbbell Pulsator , 7.66 mm. Dia. Tube.

Fig. 23 Ejector Performance with Dumbbell Pulsator and Venturi Mixing Tube, 7.66 mm Dia. Bore Tube, 345 mm Long.

Experimental Results for Ejector Driven by Piston-Cylinder Pulsator

This pulsator showed promise and was tested extensively as the results in figure 24a to 24e indicate. But, beyond about 0.3 Mach number, the minimum Mach number started going up, thereby reducing the pulsation strength. Results when both the crankcase and the exhaust duct were blocked were better than when they were open by almost 25% for the 7.66 mm dia. bore tube. The 5.05 mm dia. nozzle does not show the same improvement. This

is attributed to the emptying time being longer when a nozzle is present, which causes the minimum Mach number on the pulse to be higher.

Figure 24c shows there is a noticeable increase in P.E. as average flow Mach number increases. The R.V.P. driven ejector did not show this. Figure 24f also does not show an increase in the pulsation strength as Mj increases. P.E.R. in figure 24d shows a behavior some what like a combination of the loudspeaker acoustic driver at low Mach numbers and more like an R.V.P. at higher Mach numbers. This is of interest as the piston-cylinder pulsator has a suction part in the pulse at low flows like a loudspeaker. At higher flow rates, the pulse becomes all positive like an R.V.P..

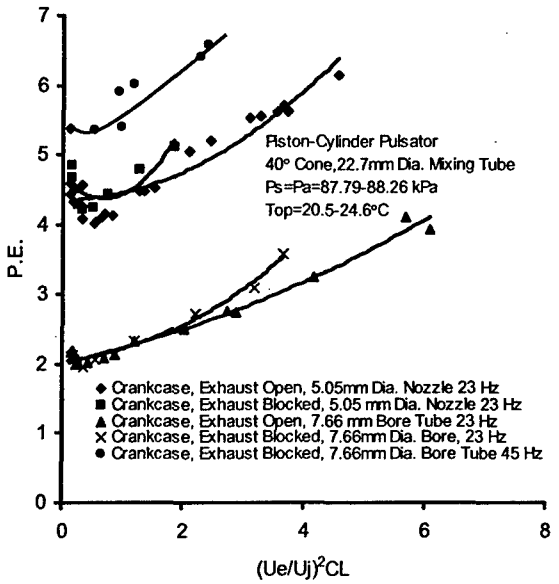

Fig. 24a Ejector Pumping Effectiveness P.E. Versus (Pulsation Strength)^{2}CL . Piston-Cylinder Pulsator 5.05 mmDia. Nozzle and 7.66 mm.Dia. Tube, 40° Cone 22.7 mm Dia. Mixing Tube.

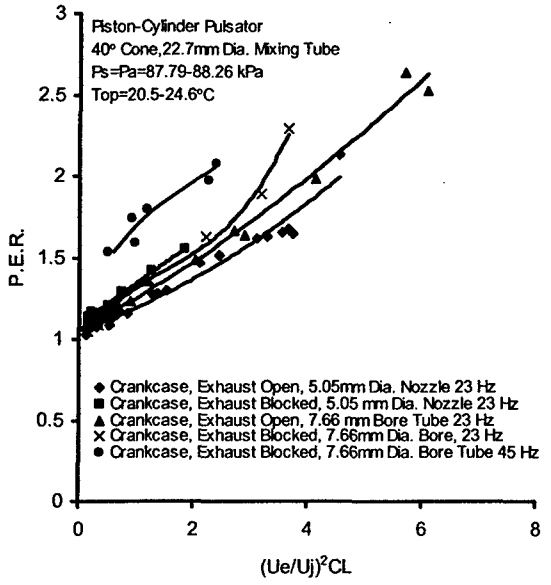

Fig. 24b Ejector Pumping Effectiveness Ratio P.E.R. Versus (Pulsation Strength)^{2}CL . Piston-Cylinder Pulsator , 5.05 mm Dia. Nozzle and 7.66 mm Dia. Tube, 40° Cone, 22.7 mm Dia. Mixing Tube.

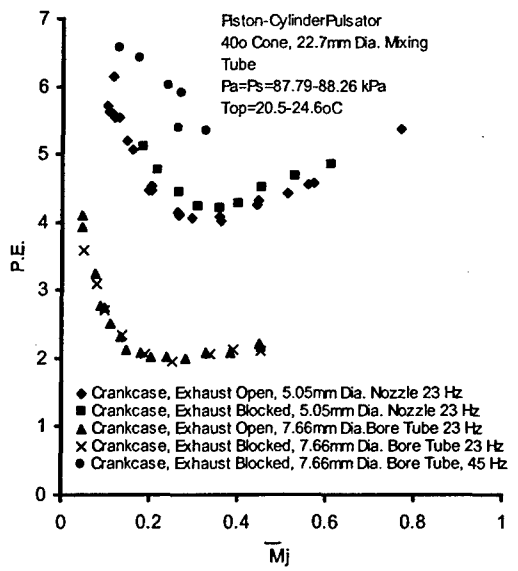

Fig. 24c Ejector Pumping Effectiveness P.E. Versus Average Jet Mach Number Mj. Piston-Cylinder Pulsator, 5.05 mm Dia. Nozzle and 7.66 mm Dia. Tube.

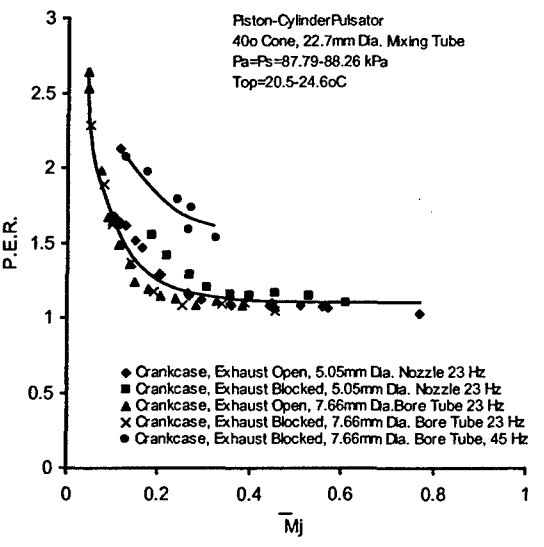

Fig. 24d Ejector Pumping Effectiveness Ratio P.E.R. Versus Average Jet Mach Number Mj. Piston-Cylinder Pulsator, 5.05 mm Dia. Nozzle and 7.66 mm Dia. Tube.

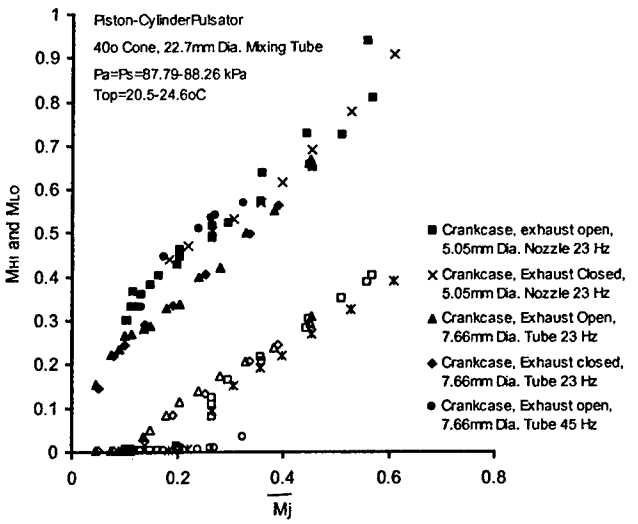

Fig. 24e Piston-Cylinder Pulsator Pulsing Effectiveness For 5.05 mm Dia. Nozzle and 7.66 mm Dia. Tube.

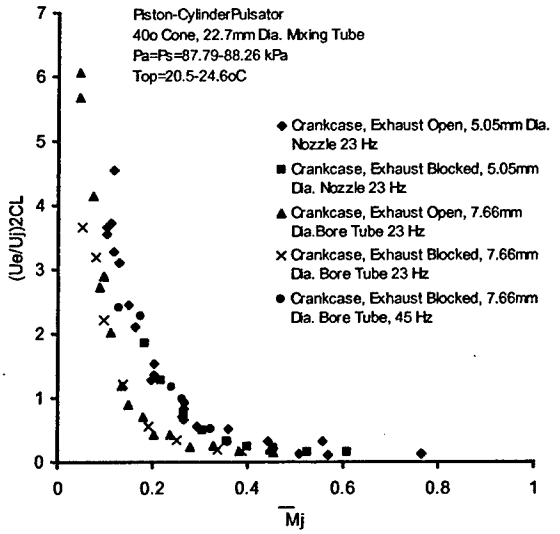

Fig. 24f (PulsationStrength)^{2}CL Versus Average Jet Mech Number. For 5.05 mm Dia. Nozzle and 7.66 mm Dia. Tube.

Fig. 24 Performance of An Ejector Driven by a Piston-Cylinder Pulsator.

Experimental Results for Ejector Driven by Synthetic Jet Actuator

Figure 16 in reference 14 shows the results obtained for a synthetic actuator. The results have been dealt with there. It is to be reiterated here that a powerful synthetic actuator would produce a pulsed jet which would be as effective as a pulsed jet with primary flow.

Computational Investigation of Pulsed Ejectors; CFD approach and Results

The 3D simulation of the ejector model was with FALCON, the CFD software being developed and used by Lockheed Martin Aeronautics Company's Fort Worth location. The geometry of the ejector analyzed was similar to

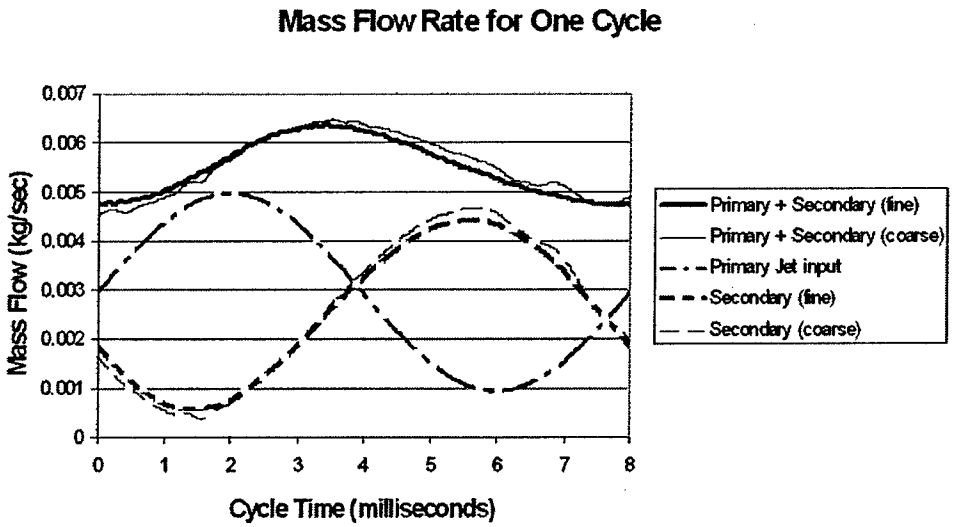

Fig. 25 Mass Flow Rates Calculated by CFD.

Both the coarse and the fine grid appear to give a -19% error in secondary flow and a -20.4% error in P.E.. that

shown in figure 7 except that the diameter of the primary nozzle was 10.03 mm. Some details of this software the results are given in figure 18 of reference 14. Relevant details of work done are given in figure 25 and table 1.

Table 1: Pulsed Ejector Results for 125 Hz, Dj = 10.03 mm, Uj_bar = 34.74 m/s, Ue = 28.2 m/s

		Coarse Grid		Fine Grid	
	Experiment	CFD	% Diff	CFD	% Diff
U_j (m/s)	41.8	40.0	-4.3	36.0	-13.9
U_j_bar (m/s)	34.74	35.16	1.2	35.78	3.0
U_e (m/s)	28.2	25.3	-10.3	24.4	-13.5
U_e/U_j	0.675	0.633	-6.2	.677	0.30
M_p (kg/s)	0.002913	0.002954	1.4	0.002949	1.2
M_s (kg/s)	0.003253	0.002638	-18.9	0.002632	-19.1
M_s/M_p	1.12	0.89	-20.5	0.89	-20.5
P_{0j}_bar (kPa)	90.55	90.52	-0.03	90.45	-0.11
P_{0s} (kPa)	89.7	89.8	0.1	89.8	0.1
P_{0t} (kPa)	90.04	90.00	-0.04	89.91	-0.14
T_{0p}_bar (deg C)	21.2	21.5	1.4	21.6	1.9
T_{0t} (K)	294.5	294.3	-0.07	294.7	0.07
$(M_s/M_p)*(P_{0j}\_bar/P_{0s})*(T_{0s}/T_{0p})^{1/2}$	1.13	0.90	-20.4	0.90	-20.4
$(U_e/U_j)^2$	0.46	0.40	-13.0	0.46	0
rho_t(kg/m^3)	1.061	1.062	0.09	1.060	-0.09
Re	24,455	23,647	-3.3	21,280	-13.0
St	0.03	0.03	0	0.03	0

Grid at Jet/Cone cross-section.

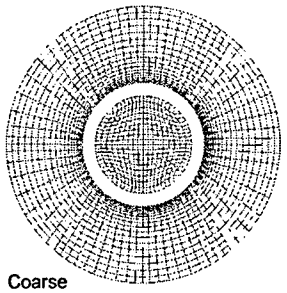

Coarse

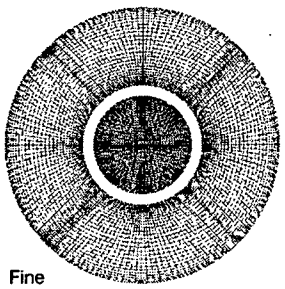

Fine

Of interest is the analysis carried out from figure 4. The velocity averaged inside the boundary of the jet gave $\overline{Uj}$=38.624 m/s so that Ue=29.666 m/s giving (Ue/Uj) CL=0.768. Mp=0.0008324 kg/s from previous measurements. This was then associated with the centerline velocities of the jet for the pulsed case and plotted. Integrating under the solid line over the area of the cone gave (Mp+Ms)WD and subtracting Mp gave (Ms)WD=0.003344 kg/s. Similarly integrating under the dashed line over the area of the cone and subtracting Mp gave (Ms)ND=0.002621 kg/s. Figure 26 shows a plot of (Ms+Mp)=M_T, (Ms)WD and Mp against time in ms. It should be noted that (Ms)WD is a maximum when Mp is a minimum and visa versa. This is accounted for by the velocity distribution in the jet when pulsed. The maximum at the jet boundary occurs when the velocity at the centre-line of the jet is a minimum and visa versa. The only comparable results available are at 40.2528 m/s, 131 Hz and for that frequency Ms(WD)=0.004218 and Ms(ND)=0.00311 kg/s. The discrepancy is due to the frequency 175 Hz not being the resonant frequency.

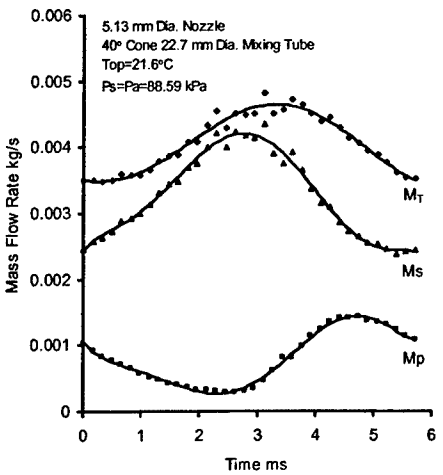

Fig. 26 Integrated Values of Ms, Mp and MT from Figure 4.

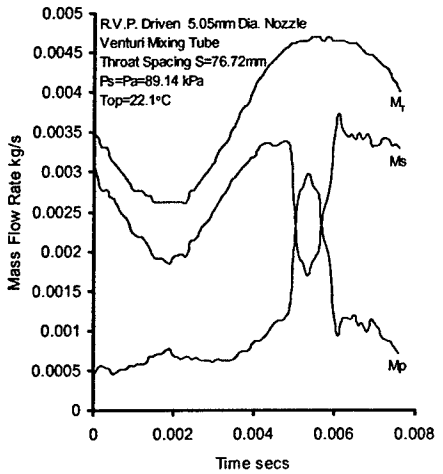

Fig. 27 Values of Mp,Ms and M_T for an R.V.P., 5.05 Nozzle Venturi Mixing Tube.

With LabView software it was possible to measure values of hotfilm anemometer voltages one diameter downstream of the nozzle and pressure drop across the measuring nozzle as shown in figure 4 at the exit of the mixing tube, as these values varied over a pulse. This was done for an R.V.P. driven 5.05 mm Dia. Nozzle with a Venturi mixing tube. Figure 27 shows a plot of Mp, Ms and M_T over a primary jet pulse cyle. The calculated P.E. was 2.71 and P.E.R. was 1.46 at 131.5 Hz. For this plot Mp was calculated from hotfilm readings and the value was 0.001012 kg/s and $\overline{Uj}$ was 47.8 m/s. Ms was measured using the orificemeter in the secondary air supply line and was 0.002695 kg/s, so that M_T from these two measurements was 0.003707 kg/s. M_T was also calculated from pressure drop across the measuring orifice one meter downstream of the mixing tube exit shown in figure 4. Ms was then calculated by subtracting Mp from M_T. Ms calculated from taking the average values of Mp and MT was 0.002715 kg/s, in good agreement with the measured value.

There is a good trend agreement between the CFD calculations and the curves shown in figures 26 and 27. It is unfortunate that direct comparable cases were not investigated. It became obvious that the 17.41 mm dia. tube was constricting the flow for a 10.03 mm dia. nozzle. In fact it was not able to accommodate even a 5.13 mm dia.nozzle.

Discussion

The ejector with 5.13 mm dia. nozzle and 21°, 30° and 40° cone with 17.41 mm dia. cylindrical tube, driven by loudspeaker as well as R.V.P. is discussed in reference 14. A loudspeaker acoustic driver, though convenient, has the shortcoming that the resonant frequency is where the maximum $(Ue/Uj)^2CL$ is obtained. This frequency is fixed by the speaker and the ejector system and tubing, altogether and cannot be altered easily so that even though the frequency of the loudspeaker itself can easily be changed, best results are achieved only at one frequency. Therefore these experiments do not provide enough data to decide the best frequency for the ejector.

It also appears that large scale turbulence in the jet flow obscures the presence of vortices and the pumping effectiveness suffers. This is particularly noticed in tests carried out with the R.V.P. and the dumbbell pulsator. At higher flows the jet flow became extremely turbulent and the performance of the ejector suffered. Figure 23b shows the steep drop in both P.E. and P.E.R. against $\overline{Mj}$ for the dumbbell pulsator.

The effect of Reynolds number and Strouhal number for the ejector with the smaller 17.41 mm dia. cylindrical tube has been discussed in reference 14. Their effect on the ejector with the bigger 22.7 mm dia. cylindrical tube appears to be the same. Figure 20 shows that P.E. decreases with increase in throat spacing S for $\overline{Uj}$=20 m/s, is almost constant for 40 m/s and decreases slightly for 91 m/s, when the 40° cone or the plate is at the mixing tube entrance. For the tube by itself the same behavior is seen, though to a smaller extent.

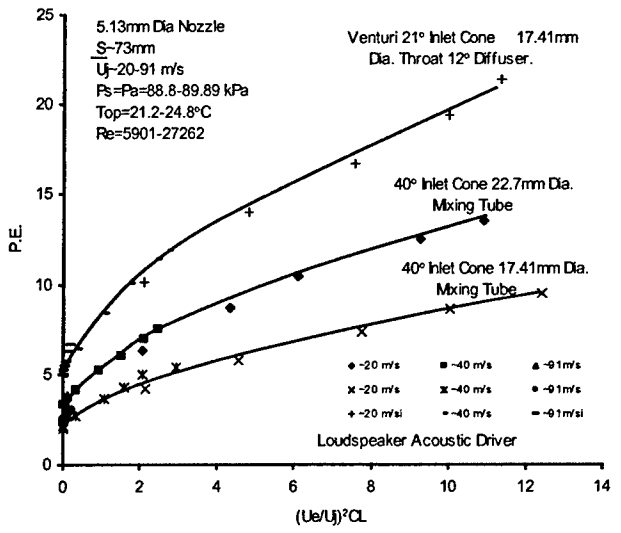

Fig. 28 Comparison of P.E. versus $(Ue/Uj)^2CL$ For a Venturi, 40o Cone with 17.41 mm Dia. tube and 22.7 mm Dia. Tube.

Figure 28 is a comparison of the ejector performance with a Venturi, 40° cone and 22.7 mm dia. tube and 40° cone and 17.41 mm dia. tube. The Venturi is the best, but the 40° cone with the bigger tube is much better than the one with the smaller tube by more than 27%. The reason for this is apparent from figure 1. The jet boundary is about 4 times diameter of the nozzle and for a 5.13 mm dia. nozzle at least a 20.52 mm dia tube is needed to accommodate the flow. A 17.41 mm dia. tube constricts the flow.Of course the Venturi is better as it lets the flow regain the pressure. As shown in figure 16, the pressure needed to drive a given mass flow rate out of the test section through a Venturi is about half that required to drive the same flow rate out through a cone and tube combination. It appears that it may even be possible, though more tests have to be made, that the pressure required to drive a given mass flow rate gives a good measure of the ejector performance.

Figures 19 and figure 9 of reference 14 show that P.E. does not change significantly with changes in the entrance configuration of the mixing tube. Thus 21°, 30°, and 40° cones with the 17.41 mm dia. tube give approximately same values of P.E. for a given $\overline{Uj}$ and throat spacing S. Also the 40° cone, the plate rounded into the 22.7 mm dia. tube give the same P.E.. It appears that the entrance shape is not important. The reason for this is again explaied by figure 1. The jet boundary in figure 1 shows that it expands to 4 times the diameter of the nozzle immediately downstream of it and then remains virtually constant. All the entrainment appears to take place in this region. That is, the initial vortex entrains the additional Ms.

The exiting shape of the mixing tube on the other hand, influences the performance of the ejector. If the exiting shape is a cylindrical tube, its diameter has to be at least 4 times the diameter of the nozzle. Even for the tube by itself without an entrance shape, the performance does not deteriorate much and the deterioration is probably due to not all of the total flow going into the tube. The Venturi is the best shape, but is difficult to make, so that a simple tube with a diameter 4 times that of the nozzle may be a good compromise if a slight performance penalty is not critical.

Results of ejector performance using a piston-cylinder pulsator, given in figure 23. At low jet flows the suction and pressure created by the piston made this pulsator behave like a loudspeaker. At higher jet velocities the velocity pulses became completely positive and the pulsator behaved like an R.V.P.. This is seen in the plot of P.E. and P.E.R. versus $(Ue/Uj)^2CL$ in figures 23a and 23b. It is also seen there that P.E. and P.E.R. are higher for the case of crankcase and exhaust ports being closed. In the beginning the exhaust was blocked, but in a way that there was a volume equal to half the swept volume present at the exhaust port. This volume was acting like a reservoir and making the bottom of the velocity pulses high. This caused poor P.E. results. With the exhaust and the crankcase blocked close to the cylinder end of the ports there was less leakage and the pulsations were sharper. This accounts for the better performance of the ejector in this condition. P.E. stayed constant or increased with $\overline{Mj}$ as in figure 23c beyond 0.2 to 0.3. This is surprising as $(Ue/Uj)^2CL$ does not appear to increase in the same interval as seen in figure 23f. Generally the piston-cylinder pulsator driven ejector appears to behave like a loudspeaker driven ejector as shown in figure 23d and figure 16 of reference 14.

The tube pulsator showed the most promise in that, the pulsation strength did not decrease as the mass flow rate increased. The losses in the pulsator appear to be fairly large and more research is needed to make it practicable.

Results of the CFD work have been included. Unfortunately as stated before most of the present work has been on a 5 mm dia. nozzle,while the CFD work is on a 10 mmdia. nozzle. Hence comparisons are difficult to make. Both CFD analysis and the experiments show that there is a time lag between Mp and Ms. In fact maximum Ms occurs when Mp is at the minimum during the pulsation. This is due to the maximum velocity at the jet boundary occurring when the velocity at the jet centre-line is a minimum.

The differences in the CFD and experimental results do not appear to improve with grid size reduction. The fine grid used appears to be more than adequate. The uniform primary jet velocity assumed in CFD calculations has been suggested as a possible reason for the discrepancies though surprisingly turbulent profiles have been reported to give worse results. This is possible as figure 4 indicates that the primary jet velocity profile is anything but uniform. Unfortunately, some parameter oscillatory problems have been encountered in the calculations leading to negative values of Mp and Ms during part of the cycle, creating low pumping effectiveness. It has been suggested that using higher input values of Mp to prevent it from going negative would also increase Ms during the cycle , thereby improving the pumping effectiveness.

Conclusions

The performance of an ejector driven by a loudspeaker acoustic driver and 5.13 mm dia. nozzle was strongest at 127-131 Hz, pulsations increased pumping effectiveness for all mixing tube geometries by up to 4.5 times relative the steady flow ejector for an input of 150 W to the speaker. The improvement appears to be caused by the high velocity at the boundary of the jet due to the vortices produced by the pulsation. Most of the entrainment appears to occur at the initial vortex immediately downstream of the nozzle. This also appears to be the reason for a mixing tube of type cone-cylindrical tube combination, the entrance geometry of the mixing tube does not appear to be important as long as prevents part of the total flow from flowing outside the tube portion. The penalty incurred by the use of a tube by itself without an entrance which would allow part of the total flow to go outside the exiting tube is not large. The exit portion of the mixing tube is important and requires the cylindrical tube portion to have a diameter at least 4 times that of the nozzle to accommodate the total flow. The performance is

improved upto 100% by the use of a Venturi as the mixing tube. There is insufficient data to decide the best frequency for the pulsator.

The performance of the disc rotor valve pulsator (R.V.P.) improved significantly by the use of a narrow velocity-time pulse. The R.V.P. ejector was better than the loudspeaker at higher jet average Mach numbers. The performance of the dumbbell pulsator was very unsatisfactory, mainly due to frequency restrictions and extreme turbulence. The piston-cylinder pulsator provided good results and needs to be tested further. It compares well with the R.V.P. and provides a wider range of average jet Mach numbers but is limited in its frequency range.

Of the pulsator tests conducted, the Tube pulsator shows the most promise. Future work is needed to achieve better control of frequency and pulsation strength. Presently it does have the problem of air passing through very small annular space which may cause tremendous pressure losses .No pulsator tested was able to provide a square of pulsation strength $(Ue/Uj)^2$ of 1.0 at an average jet Mach number of 0.5.

Recommendations

1. The loudspeaker acoustic driver behaves well, but cannot handle high pressures encountered at high Mach numbers. More robust speakers with metal bellows need to be looked at.
2. It is essential that research is done to find a pulsator which can give a pulsation strength of at least 1.0 at an average primary jet Mach number of 0.5, with minor flow losses.
3. The synthetic jet looks very feasible. A more powerful one than the one tested here needs to be researched.
4. It is evident that pulsing the primary jet does improve the ejector performance. More effort needs to be spent on a way to do this without incurring major flow losses.

Acknowledgement/Disclaimer

This work was sponsored (in part) by the Air Force Office of Sceintific Research, USAF, under grant/contract number F49620-02-1-0131. The AFOSR programme manager was Dr. Thomas J. Beutner. The views and conclusions contained herein are those of the authors and should not be interpreted as necessarily representing the official policies or endorsements, either expressed or implied, of the AFOSR or the U.S. Government. The experimental effort was strongly supported by Mr. N. Vogt, Chief Technical Supervisor; Mr. G. East, Mr. J. Mcneely and Mr. M. Johnson, Technicians, Dept. of Mechanical and Manufacturing Engineering.

The sad demise of Dr. P.J. Vermeulen on 20 Dec 2004, the chief investigator and contract holder is acknowledged.

References

1. Anderson, A.B.C., "A Jet-Tone Orifice Number for Orifices of Small Thickness–Diameter Ratio," *The Journal of Acoustical Society of America*, **26**, 1954, pp. 21-25.
2. Hill, W.G. and Greene, P.R., "Increased Turbulent Jet Mixing Rates Obtained by Self-Excited Acoustic Oscillations," *ASME Journal of Fluids Engineering*, **99**, No. 3, Sept. 1977, pp. 520-525.
3. Vermeulen, P.J. and Yu, Wai Keung, "An Experimental Study of the Mixing by an Acoustically Pulsed Axisymmetrical Air-Jet," *International Journal of Turbo and Jet-Engines*", **4**, Nos. 3-4, 1987, pp. 225-237. First published at *30th ASME International Gas Turbine Conf.*, Houston, TX, March 18-21, 1985, Paper No. 85-GT-49.
4. Vermeulen, P.J., Ramesh, V. and Yu, Wai Keung, "Measurements of Entrainment by Acoustically Pulsed Axisymmetric Air Jets," *Trans. ASME, Journal of Engineering for Gas Turbines and Power*, **108**, No. 3, July 1986, pp. 479-484.
5. Wilson, J.,"A Simple Model of Pulsed Ejector Thrust Augmentation", NASA/CR-2003-212541
6. Vermeulen, P.J. and Ramesh, V.,"NO_x Measurements for Combustor with Acoustically Controlled Primary Zone", Trans. ASME Journal of Engineering for Gas Turbines and Power, Vol. 119, No. 3, July 1997, pp. 559-565.
7. Vemeulen, P.J., Rainville, P. and Ramesh, V., "Measurements of the Entrainment Coefficient of Acoustically Pulsed Axisymmetric Free Air jets," *Trans. ASME Journal of Engineering for Gas Turbines and Power,* **114**, No. 2, April 1992, pp. 409-415.
8. Holdeman, J.D. and Walker, R.E., "Mixing of a Row of Jets with a Confined Crossflow," *AIAA Journal,* **15**, 1977, pp. 243-249.

9. Vermeulen, P.J., Chin, Ching-Fatt and Yu, Wai Keung, "Mixing of an Acoustically Pulsed Air jet with a Confined Crossflow," *AIAA Journal of Propulsion and Power,* **6**, No. 6, 1990, pp. 777-783.
10. Vermeulen, P.J., Grabinski, P. and Ramesh, V., "Mixing of an Acoustically Excited Air jet with a Confined Hot Crossflow," *Trans. ASME, Journal of Engineering for Gas Turbines and Power,* **114**, No. 1, January 1992, pp. 46-54.
11. Yu, Wai Keung, "An Experimental Study of the Mixing Behavior of Acoustically-Pulsed-Air Jets," M.Sc. Thesis, University of Calgary, Mechanical Engg. Dept., Canada, 1985, pp. 99.
12. Parikh, P.G., Moffat, R.J., "Mixing Improvement in a Resonantly Pulsed, Confined Jet," *ASME Fluid Mechanics of Combustion Systems,* Morel, T., Lohmann, R.P., Rackley, J.M., (Editors), Fluids Engg. Conf., Boulder, Colorado, 22-23 June, 1981, pp. 251-256.
13. Anderson, A.B.C., "Vortex-Ring Structure-Transition in a Jet Emitting Discrete Acoustic Frequencies," *The Journal of the Acoustical Society of America*, **28**, No. 5, September 1956, pp. 914-921.
14. Vermeulen, P.J., Ramesh, V., Meng, G.C., Miller, D.N., Domel, N., "Air Ejector Pumping Enhancement Through Pulsing Primary Flow", 2nd AIAA Flow Conference, 28 June-1 July 2004, Portland, Oregon, AIAA 2004-2621.
15. Miller, D.N., Yagle, P.J. and Hamstra, J., "Fluidic Throat Shewing for Thrust Vectoring in Fixed-Geometry Nozzles," *AIAA Paper 99-0365,* 1999.
16. Yagle, P.J., Miller, D.N., Ginn, K.B. and Hamstra, J.W., "Demonstration of Throat Skewing for Thrust Vectoring in Structurally Fixed Nozzle," *ASME Paper 2000-GT-0013*, May 2000.
17. Miller, D.N., Yagle, P.J., Bender, E.E., Ginn, K.B. and Smith, B.R., "Pulsed Injection for Nozzle Throat Area Control," Final Technical Report, AFOSR No. F49620-98-C-0016, March 2001.
18. Ramesh, V., Vermeulen, P.J. and Munjal, J.L., "Measurement of Acoustic Power for a Tube Air Flow and Correlation with Exit Pulsation Velocity," *Proc. Inter-Noise '93, II,* Leuven, Belgium, 1993, pp. 1227-1230.
19. Der, J.,"Improved Methods of Characterizing Ejector Pumping Performance", AIAA 27th Aerospace Sciences Meeting, Reno, Nevada, 1989, AIAA 89-0008, pp. 1-12.

Appendix 1

Table 1

Ejector Performance Tests with 5.13mm Dia. Nozzle , Loudspeaker Acoustic Driver in Large 285 L Enclosure

Primary Jet Velocity m/s	Frequency Hz	Mixing Tube Geometry	Throat Spacing S mm	Number of Tests
0,20,40,55,75,91	131	30° Cone Entrance-17.41mm Dia. 153.2mm long Cylindrical Tube	11.17,18.86,36.79 56.13,76.72	6 per Velocity - 6 per S 180 Tests
20	249	As Above	18.86	6 Tests
0,20,40,55,76	249	As Above	36.79	30 Tests
0,20	249	As Above	56.13,76.72	24 Tests
0,20,40,54	244	As Above	18.86	24 Tests
0,20,40,55,75,91	131	21° Cone Entrance-17.41mm Dia. 153.2mm long Cylindrical Tube	35.67,76.72	72 Tests
		Standard Venturi		

0,20,40,55,75,91	131	Mixing Tube, 17.41mm Throat, 46mm dia. Exit	35.67,76.72	72 Tests
0,20,40,55,75,91	131	Bellmouth with 17.41mm Dia. Cylindrical Tube	36.81,76.72	72 Tests
0,20,40,55,75,91	131	40° Cone Entrance- 17.41mm Dia. 153.2mm long Cylindrical Tube	35.67,76.72	72 Tests
0,20,40,91	131	40° Cone Entrance- 22.7mm Dia. 202mm long Cylindrical Tube	30.4,55,72.9	72 Tests
0,20,40,91	131	101.6mm Dia. Plate Entrance Rounded into 22.7mm Dia. 202mm long Cylindrical Tube	9.3,13.9,25.3,44,64.4, 102	144 Tests
0,20,40,91	131	22.7mm Dia. 202mm long Cylindrical Tube	10,18,36,74.6	96 Tests

Table 2

Ejector Performance Tests with 5.13mm Dia. Nozzle , Loudspeaker Acoustic Driver in Small 85 L Enclosure

Primary Jet Velocity m/s	Frequency Hz	Mixing Tube Geometry	Throat Spacing S mm	Number of Tests
0,20,40,55,75	20	30° Cone Entrance- 17.41mm Dia. 153.2mm long Cylindrical Tube	18.86	30 Tests
0,20,40,55,75,91	127	30° Cone Entrance- 17.41mm Dia. 153.2mm long Cylindrical Tube	18.86	36 Tests

Table 3

Ejector Performance Tests, 5.13mm Dia. Nozzle, R.V.P. Driver with 19.05mm Dia. Rotor Holes

Primary Jet Flow Average MachNumber	Frequency Hz	Mixing Tube Geometry	Throat Spacing S mm	Number Of Tests
0.1248-0.8569	106-328	30° Cone Entrance- 17.41mm Dia. 153.2mm long Cylindrical Tube	36.79	14 Tests

Table 4

Ejector Performance Tests- Other Pulsators

Primary Jet Flow Average MachNumber	Frequency Hz	Pulsator	Nozzle Geometry	Mixing Tube Geometry	Throat Spacing S mm	Number Of Tests
0.0309-.10509	40	Dumbbell	7.66mm Dia. Bore Tube	Venturi	76.72	7 Tests
0.102-0.7671	23 & 45	Piston-Cylinder	5.05mm Dia. Nozzle 7.66mm Bore Tube	40o Cone 22.7mm Dia. Tube	30.4	31 Tests 31 Tests

Table 5

Ejector Performance Tests, R.V.P. Driver with 6.35mm Dia. Holes into 30° Cone,17.41mm Dia. 153.2mm Long Cylindrical Mixing Tube

Primary Jet Flow Average MachNumber	Frequency Hz	Hole Geometry	Nozzle Geometry	Throat Spacing S mm	Number Of Tests
0.072-0.328	~130	6.35 mm Dia Sharp Edged	7.66mm Dia. Bore Tube	36.79	18 Tests
0.0625-0.262	210-269	As Above	As Above	As Above	10 Tests
0.056-0.289	130	As Above	As Above	As Above	10 Tests
0.0266-0.217	216	As Above	As Above	As Above	15 Tests
0.0677-0.268	256	As Above	As Above	As Above	8 Tests
0.0359-0.136	130	6.35 mm Dia. Radiused Entrance	As Above	As Above	12 Tests
0.0696-0.4688	130	6.35mm Dia Holes Radiused Entrance Rounded Exit	7.66mm Dia. Tube 3.26mm Dia Nozzle	As Above	14 Tests
0.0655-0.291	130	As Above	Long 7.66mm Dia Bore Tube	As Above	9 Tests
0.0563-0.510	130	As Above	Long 7.66mm Dia Tube,6.35mm Dia Nozzle	As above	8 Tests

Appendix 2

ENERGY CONSIDERATIONS FOR AN AIR EJECTOR

STEADY JET:

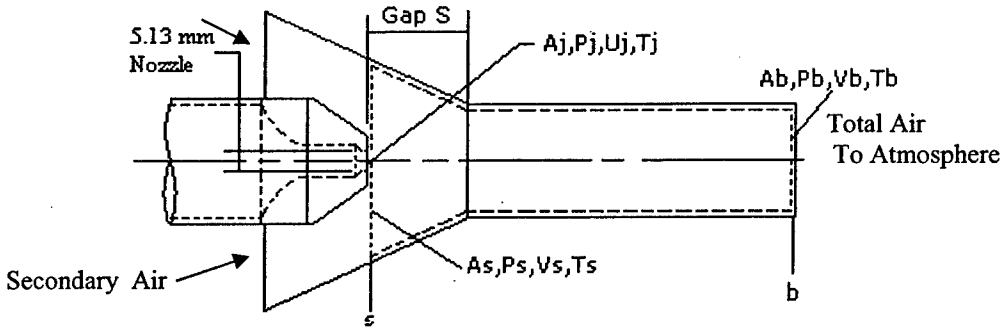

Figure 1: Control Volume Considered

Applying Steady State, Steady Flow Energy Equation to the Control Volume bounded by the nozzle exit plane and the mixing tube exit plane as shown in figure 1,

$$Mp(CpTj+1/2\,\overline{Uj}^{2})+Ms(CpTs+1/2Vs^{2})=(Mp+Ms)(CpTb+1/2Vb^{2}) \qquad (1)$$

Where Cp is the Specific Heat at Constant Pressure.
Since a horizontal ejector is being considered all potential energy terms are absent.
In experiments carried out in this laboratory, the ejector was surrounded by a test section to which entrained or secondary air was introduced to hold the test section at atmospheric pressure for all experiments. Top and Tos were measured. Mp was measured using an orificemeter.

For a specified Vs, corresponding Mach number Mss can be approximately calculated based on Tos and iterated to obtain a more accurate Mss. From this and Pos and ρ_{os}=Pos/RTs, using isentropic equations, Ps , Ts and ρ_s become available. The exit pressure of the primary jet is then Ps. Also entrainment massflow rate $Ms=\rho_s AsVs$.

Now Tb can approximated by Tb=(MpTj+MsTs)/(Mp+Ms) . From this $\rho b = Pa/RTb$ and $Vb=(Mp+Ms)/\rho_b Ab$. Therefore for this specified value of Vs equation (1) can be evaluated. The correct value of Vs can be iterated to satisfy equation (1). Once Vs is known Ms, the entrainment massflow rate can be found. As Poj and Pos are available during isentropic calculations, the Pumping Efficiency P.E. can also be found. Thus for a steady jet, it is possible to determine the entrainment masflow rate and Pumping Efficiency for the given conditions.

A computer program was written to calculate Vs and Ms for input Mp and other ambient conditions. Table 1 shows values of experimental and theoretical Pumping efficiency P.E for the same conditions. The results are for a 5.13mm Dia. Nozzle, 40° Cone with 22.7mm Dia. Mixing tube. The theoretical values are slightly higher.

Table 1

Primary Velocity m/s	Experimental P.E.	Theoretical P.E.
20.044	3.841	4.01
40.2528	3.840	4.22
91.663	3.973	4.32

PULSED PRIMARY JET:

Pulsation will be considered sinusoidal, as a majority of experimental data available is in this category.

At any instant of time when the sinusoidal pulsation has described an angle θ, the velocity of the primary jet is, Velocity= $\overline{Uj}$ +Ue sin(θ) , where Ue is the maximum amplitude of velocity pulsation above the average jet flow velocity. The kinetic energy of the primary jet flow is then,

Kinetic Energy=1/2 ρjAj($\overline{Uj}$ +Ue sin(θ))^3

The average kinetic energy is obtained by integrating the sine wave over a cycle and dividing by 2π which gives : Average Kinetic Energy=1/2 ρjAj ($\overline{Uj}^3$+1.5UjUe ^{2}).

ρjAjUj =Mp and remains constant as it is controlled by a choked valve. Hence

Average Kinetic Energy=1/2 Mp ($\overline{Uj}^2$+1.5Ue ^{2}).

The pulsed jet can now be treated as a steady primary jet, but with a velocity = ($\overline{Uj}^2$+1.5Ue ^{2})$^{1/2}$.

It is assumed at this point that the mixing between the primary and the entrained flows is completed quickly so that loss due to the shear layer between the two flows is small. The following other losses are considered.

1) Secondary flow at the entrance to the mixing tube cone = 0.32*Ms*(Vb^2)/2000 kJ

It has been assumed that secondary flow enters the cone from an infinite area.

2) Secondary flow through the contraction of the cone. For the 40° Cone in these calculations the loss = 0.0333*Ms*(Vb^2)/2000 kJ.

3) frictional loss of total flow through the mixing tube =f*(Mp+Ms)*(L/D)*((Vb/)^2)/2000 kJ (L/D) =(Gap S)/D+9. All straight tube lengths have been made to be 9D. f is to be calculated from Moody's diagram for Reynolds number Re = 4*(Mp+Ms)/πμD. In the present calculations f was calculated from

f=64/Re for .Re<2300 and ($1/f^{1/2}$)= -1.8log((6.9/Re)+(K/3.7)$^{1.11}$), where K= Relative Roughness for Re>2300.

4) loss due to total flow exiting the mixing tube = (Mp+Ms)*(Vb^2)/2000 kJ.

Equation 1 , including these losses can now be written as

$Mp(CpTj+1/2\ \overline{Uj}^2)+Ms(CpTs+1/2Vs^2)=(Mp+Ms)(CpTb+1/2Vb^2)$ +losses **(2)**

A computer programme containing these losses was written to iterate the value of Vs to satisfy this equation. Results are shown in figure 2, where experimental and calculated values of Pumping Effectiveness are plotted against the square of the pulsation strength $(Ue/Uj)^2$ for 20, 40 and 91 m/s primary jet velocities.. These results are for a 40° cone with a 22.7 mm. Dia. Smooth Mixing tube (K=0) and 5.13 mm Dia. nozzle. The gap S=30.4 mm. It is evident that there is reasonable agreement inspite of simplistic loss calculations especially regarding the pulsed flow. As pulsation strength increases the agreement between theoretical and experimental values worsens.

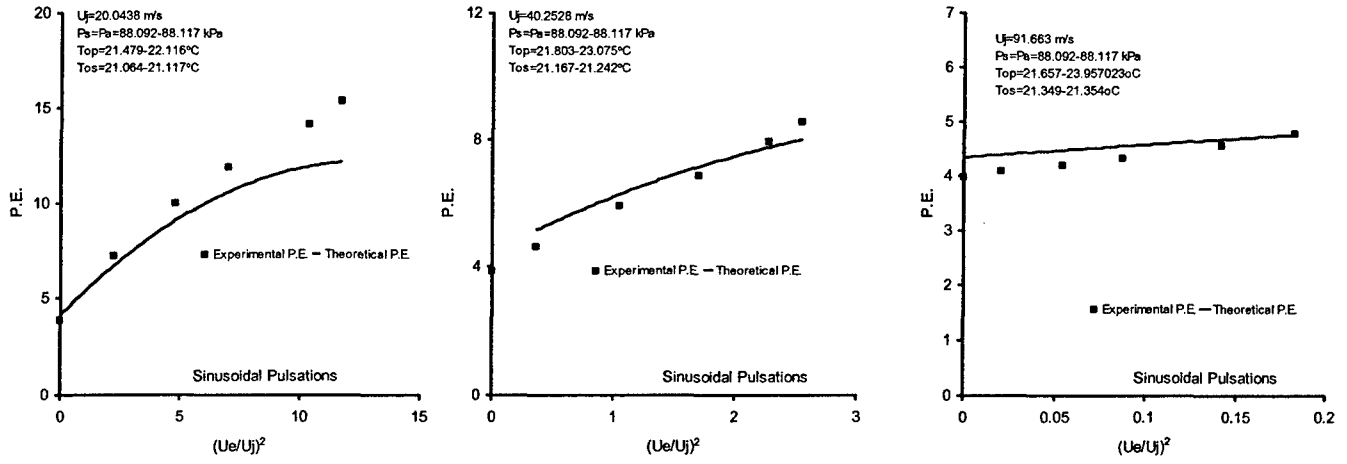

Figure 2. Experimental and Theoretical P.E. at $\overline{Uj}$ =20,40 and 91 m/s.
40° Cone, 22.7mm Dia. Mixing tube, 5.13mm Dia. Nozzle S=30.4.

Figure 3 shows experimental and calculated values of P.E. for 5.13mm Dia. Primary nozzle and a 30° cone with 17.41mm Dia. Steel Mixing tube (K=.001). Loss (2) has been corrected for the cone angle to 0.02*Ms*(Vb^2)/2000 kJ.

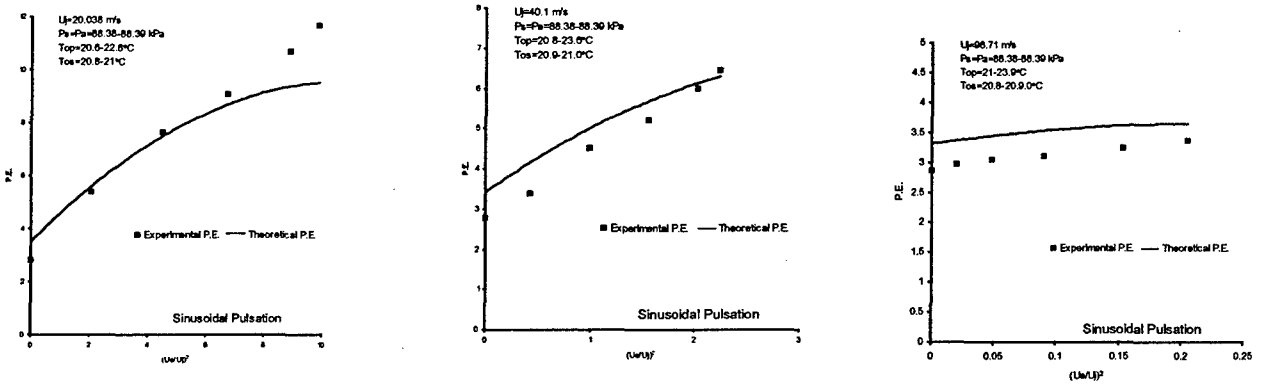

Figure 3. Experimental and Theoretical P.E. at $\overline{Uj}$ =20,40 and 98 m/s.
30° Cone, 17.41mm Dia. Mixing tube, 5.13mm Dia. Nozzle S=18.86mm.

It is evident in both figure 2 and 3, there is atleast a ball-park agreement between experimental and calculated pumping effectiveness P.E..Losses in Kinetic Energy have been treated simply, even for pulsed flows. This may account for the differences. It appears that the theory calculates slightly higher values of P.E. for steady flow which reduces as $(Ue/Uj)^2$ increases, leading to the conclusion that the losses considered for steady flows are a little too low and for pulsed flows, too high.

Appendix 3

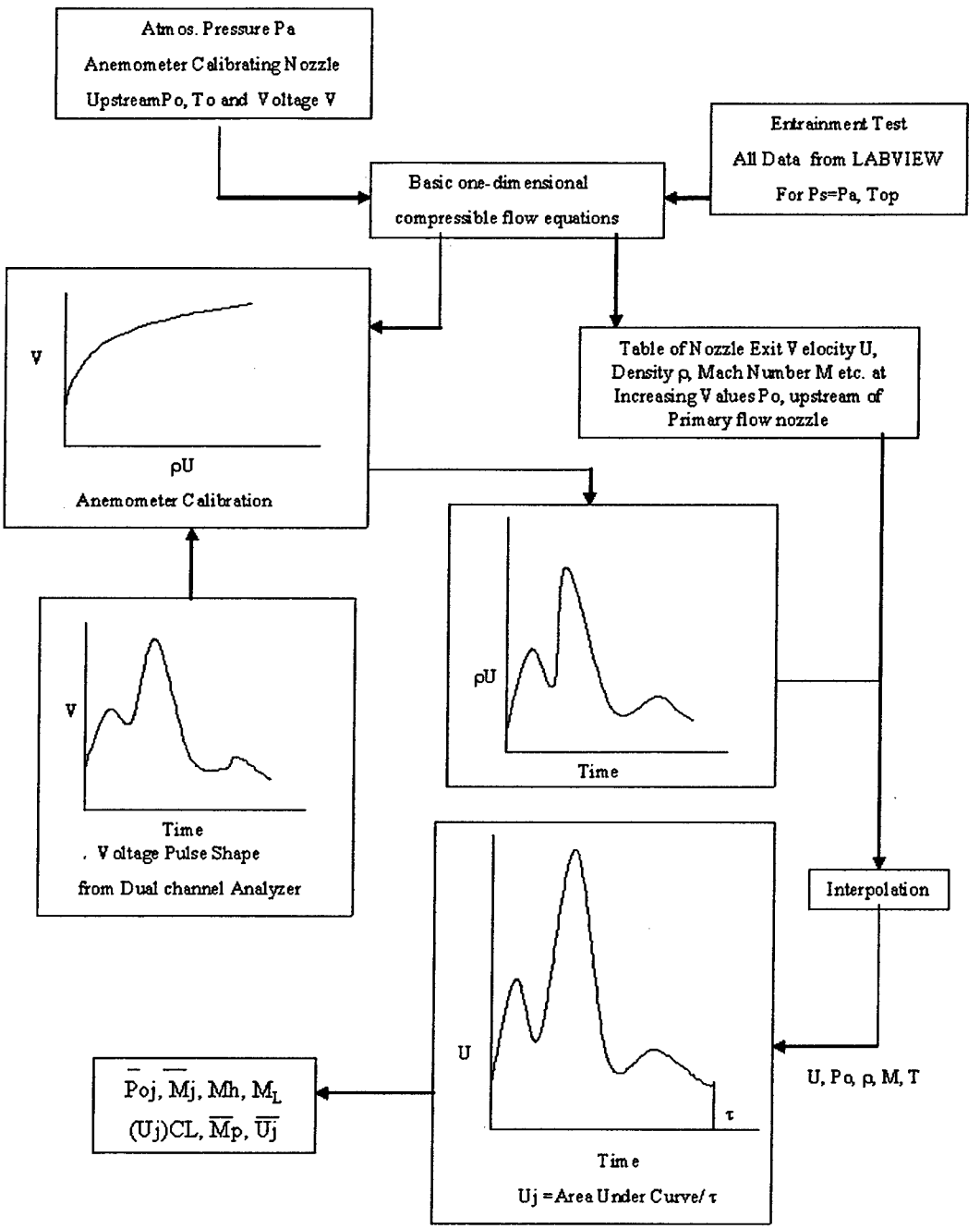
Atmos. Pressure Pa
Anemometer Calibrating Nozzle
UpstreamPo, To and Voltage V
Entrainment Test
All Data from LABVIEW
For Ps=Pa, Top
Basic one-dimensional
compressible flow equations
V
ρU
Anemometer Calibration
Table of Nozzle Exit Velocity U,
Density ρ, Mach Number M etc. at
Increasing Values Po, upstream of
Primary flow nozzle
ρU
Time
V
Time
. Voltage Pulse Shape
from Dual channel Analyzer
Interpolation
U
τ
Time
Uj =Area Under Curve/ τ
U, Po, ρ, M, T
Poj, Mj, Mh, ML
(Uj)CL, Mp, Uj